

Handbook on Lattice Green's functions

Andriy Zhugayevych (ORCID: 0000-0003-4713-1289)

December 27, 2024

1	Lattices and their Green's functions	1
1.1	Definitions	1
1.2	One-dimensional lattice	2
1.3	Fourier transform	3
1.4	Primitive lattices	4
1.5	Continual and large-scale approximations	5
1.6	Path expansion	7
1.7	Recurrence formulas and series at singularities	9
1.8	Evaluation of lattice Green's functions	10
2	Hypercubic lattice	11
2.1	General statements	11
2.2	Path expansion	12
2.3	Recurrence relations and series at $s = 0$	13
2.4	Large-scale approximation	15
2.5	Periodic hypercubic lattice	16
2.6	Square lattice	17
2.7	Simple cubic lattice	18
3	Other lattices	19
3.1	Triangular lattice	19
3.2	Face-centered cubic lattice	21
3.3	Diamond lattice	21
3.4	Body-centered cubic lattice	21
3.5	Anisotropic lattices	22
4	Appendix	22
4.1	Some properties of finite difference operators	22
4.2	Estimates and inequalities for Green's function for $s \geq 0$	22
4.3	Finite and semi-infinite one-dimensional lattices	23
4.4	Some properties of complete elliptic integrals	23
4.5	Series at $s = 0$ for hypercubic lattice: implementation	24

Preface

See the project webpage at <https://cmsos.github.io/lgf/>. References to procedures from LatticeTools package (<https://zhugayevych.me/maple/LatticeTools/>) are marked as [procedure_name]. Main ideas of this work have been published in [Zhugayevych25a].

§1. Lattices and their Green's functions

1.1. Definitions

Graph is a collection of points (enumerable set X) and bonds (subset of symmetrized X^2) with finite coordination number, which is the maximum number of bonds attached to a point (i.e. simple undirected finite-dimensional graph). In what follows we consider only connected graphs and denote a graph simply by the set of its points X . The bonding between points establishes the metrics $|\cdot|$ as the length of the shortest path between two points: $|x - y|$. If a graph can be immersed in \mathbb{R}^d in such a way that the minimum distance between its points is nonzero and the maximum length of its bonds is finite then the minimum d is called

dimension of the graph (an example of infinite dimensional graph is a tree). The Euclidean metrics in \mathbb{R}^d is denoted by $\|x - y\|$. *Lattice* is a finite dimensional graph whose all points are equivalent (i.e. for any two points or bonds there exists graph automorphism transforming them into each other). A lattice is called *isotropic* if all its bonds are also equivalent (an example of anisotropic lattice is **hcp** lattice). A lattice is called *primitive* if all its points are translationally equivalent (e.g., **sc**, **tri**, **fcc**, **bcc**).

Laplace operator on X is defined as

$$(\Delta f)_x = \sum_{z: |x-z|=1} (f_z - f_x) \equiv \sum_{z: |x-z|=1} f_z - w_x f_x,$$

where w_x is the *coordination number* of the point x . Here and below a sum without limits means the sum over X and a sum over $|x - z| = 1$ means the nearest neighbor sum. *Lattice Green's function* is a resolvent of the Laplace operator:

$$g(s) = (s - \Delta)^{-1}. \quad (1.1)$$

It satisfies the equation

$$s g_{yx} - \delta_{yx} = \sum_{z: |x-z|=1} (g_{yz} - g_{yx}). \quad (1.2)$$

Because the bonds are undirected $g_{xy} = g_{yx}$. Note that the inverse Laplace transformation of the lattice Green's function, $\tilde{g}(t)$, obeys the equation $\dot{\tilde{g}} = \Delta \tilde{g}$ with $\tilde{g}(0) = \delta$.

From the general theory of Markov chains it follows that the spectrum of the Laplace operator on a graph is real and lies within the segment $[-2w_{\max}, 0]$, where $w_{\max} = \max_x w_x$. Here $s = 0$ is the eigenvalue with eigenvector $f_x = 1$ and multiplicity equal to the number of connected components of the graph. Any regular infinite lattice of equivalent points can be partitioned into a finite number of equivalent sublattices so that each sublattice has no bonds between its points. Examples: **sc** and **bcc** into 2 **sc**, **gra** into 2 **tri**, **tri** into 3 **tri**, **fcc** into 4 **sc**, **dia** into 2 **fcc**. If p is the minimum number of such sublattices then $w_0 p / (1 - p)$ is the leftmost eigenvalue with eigenvector $f_x = \exp(i2\pi k/p)$, where $k = 1, \dots, p$ is the index of the sublattice containing the point x . In particular, the Green's function of a bipartite lattice is odd or even function of an argument $s - w_0$ depending on sublattice, namely

$$g_x(s) = (-1)^{|x|+1} g_x(-s - 2w_0). \quad (1.3)$$

At the branch cut Green's function is defined as follows

$$g^\pm(s) = g(s \pm i0).$$

We assume $g = g^+$, then $g^- = \bar{g}$. The density of states

$$\rho_x(\sigma) = -\frac{1}{\pi} \Im g_{xx}(-\sigma). \quad (1.4)$$

Lattice bond Green's function is defined for a pair of directed bonds $(x \rightarrow x')$ and $(y \rightarrow y')$ as follows

$$g_{(x,x')(y,y')} = g_{x'y} + g_{xy'} - g_{xy} - g_{x'y'}, \quad (1.5)$$

that is the special second order difference expression.

1.2. One-dimensional lattice

The case $X = \mathbb{Z}$ can be analyzed in details:

$$g_x = g_0 \alpha^{|x|}, \quad (1.6)$$

where

$$g_0(s) = \frac{1}{\sqrt{s(s+4)}} \equiv \frac{q}{2\sqrt{1-q^2}}, \quad \alpha(s) = 1 + \frac{s}{2} - \sqrt{s\left(1 + \frac{s}{4}\right)} \equiv \frac{q}{1 + \sqrt{1-q^2}}.$$

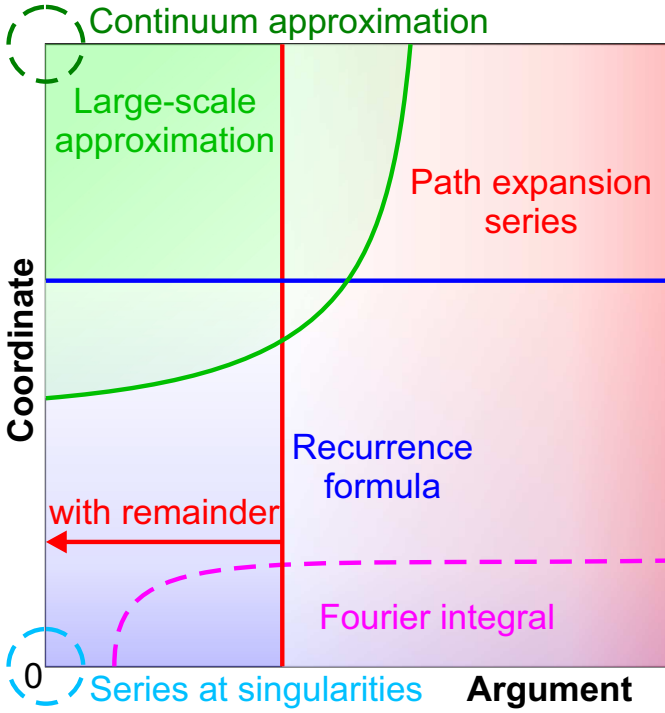


Figure 1: Methods available for efficient evaluation of the Green's function of a lattice with root-free dispersion $S_\mu(k)$.

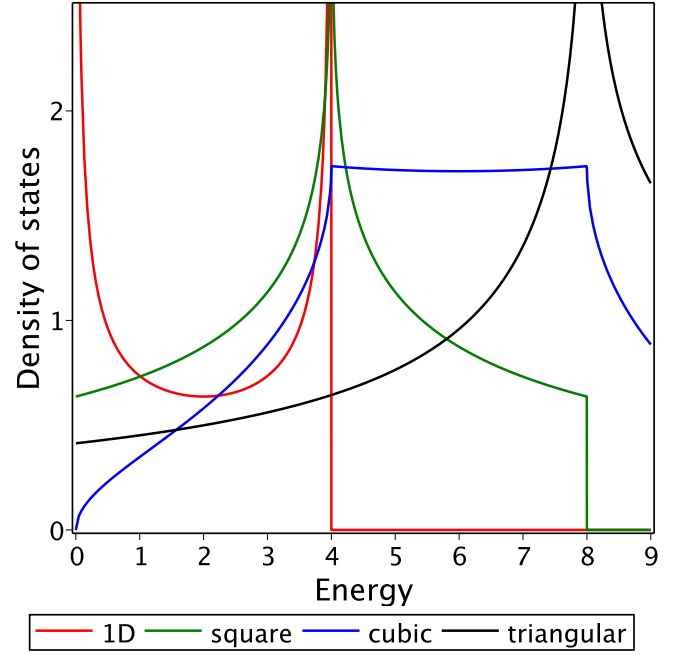


Figure 2: Density of states rescaled by the bandwidth for several lattices discussed in the text.

We have four alternative variables: s , q , α , and $\kappa = -\ln \alpha$. Here are relations between them:

$$\begin{aligned} \alpha^{\pm 1} &= 1 + \frac{s}{2} \mp \sqrt{s \left(1 + \frac{s}{4}\right)} \equiv \left(\frac{\sqrt{s+4} \mp \sqrt{s}}{2}\right)^2, & \tilde{\alpha}(t) &= \frac{g_1(t)}{t}, \\ s+2 &= \frac{2}{q} = \alpha + \alpha^{-1} = 2 \cosh \kappa, & s &= \frac{(1-\alpha)^2}{\alpha}, & s+4 &= \frac{(1+\alpha)^2}{\alpha}, \\ g_0 &= \frac{\alpha}{1-\alpha^2} = \frac{1}{2 \sinh \kappa} = (-\ln \alpha)', & g_x &= \left(-\frac{\alpha^x}{x}\right)', & 2g_1 &= \frac{1}{\sqrt{1-q^2}} - 1. \end{aligned}$$

At the branch cut

$$g_0(s) = \frac{-i}{\sqrt{-s(s+4)}} \implies \rho(\sigma) = \frac{1}{\pi \sqrt{\sigma(4-\sigma)}} \quad (1.7)$$

and

$$s = -4 \sin^2 \frac{k}{2} \pm i\epsilon, \quad \kappa = \pm ik + \frac{\epsilon}{2 \sin k}, \quad \alpha = e^{-\kappa}.$$

The propagator

$$\tilde{g}_x(t) = e^{-2t} I_x(2t), \quad (1.8)$$

where I is the modified Bessel function. It satisfies the following recurrence relations:

$$\dot{\tilde{g}}_x = \tilde{g}_{x-1} + \tilde{g}_{x+1} - 2\tilde{g}_x, \quad x\tilde{g}_x = t(\tilde{g}_{x-1} - \tilde{g}_{x+1}). \quad (1.9)$$

Finite and semi-infinite one-dimensional lattices are considered in Section 4.3.

1.3. Fourier transform

Points of a lattice can be enumerated by pairs (ξ, α) , where $\xi = (\xi_1, \dots, \xi_d)$ is the coordinate of the unit cell, which is the translationally invariant piece of the lattice of a minimum size, and $\alpha = \overline{1, \nu}$ enumerates points within the unit cell (e.g., for primitive lattices $\nu = 1$, for gra and dia lattices $\nu = 2$). Coordinates $\xi_i \in \mathbb{Z}$ for

infinite lattice and $\xi_i = 0, \dots, L_i - 1$ for torus. This enables us to use Fourier transform for solving (1.2), which for a function $f_x = f_\xi^\alpha$ is defined as

$$\hat{f}^\alpha(k) = \sum_{\xi} f_\xi^\alpha e^{ik\xi}, \quad (1.10)$$

where $k\xi = \sum_{i=1}^d k_i \xi_i$. Its inverse for infinite lattice is given by

$$f_\xi^\alpha = \frac{1}{(2\pi)^d} \iint_{-\pi}^{\pi} \hat{f}^\alpha(k) e^{-ik\xi} dk, \quad (1.11)$$

here and below we use shortcut notations for d -dimensional integrals over $[-\pi, \pi]^d$. Generally the most efficient way to compute Fourier integrals is to approximate it by a finite sum over a regular k -grid with a proper symmetry [Morgan20]. The simplest grid approximates an infinite lattice by torus:

$$f_\xi^\alpha = \frac{1}{L_1 \dots L_d} \sum_k \hat{f}^\alpha(k) e^{-ik\xi}, \quad k_i = \frac{2\pi(l_i + \lambda_i)}{L_i}, \quad l_i = 0, \dots, L_i - 1, \quad (1.12)$$

where λ_i are shifts of the grid. By presenting Green's function as $g_{yx} = g_{\xi-\eta}^{\beta\alpha}$, where $x = (\xi, \alpha)$ and $y = (\eta, \beta)$, and applying Fourier transform to (1.2) we obtain a set of linear algebraic equations of the order ν :

$$s\hat{g}^{\beta\alpha} - \delta^{\beta\alpha} = \sum_{\zeta, \gamma: |\zeta+\gamma-\alpha|=1} \left(e^{-ik\zeta} \hat{g}^{\beta\gamma} - \hat{g}^{\beta\alpha} \right). \quad (1.13)$$

By solving Eq. (1.13) and using the inverse Fourier transform (1.11) one can get the Green's function. Since \hat{g} is a nondefective matrix

$$\hat{g} = \sum_{\mu=1}^{\nu} \frac{P_\mu(k)}{s - S_\mu(k)} \implies g_\xi^{\beta\alpha}(s) = \sum_{\mu=1}^{\nu} g_{\xi;\mu}^{\beta\alpha}(s), \quad g_{\xi;\mu}^{\beta\alpha}(s) = \frac{1}{(2\pi)^d} \iint_{-\pi}^{\pi} \frac{P_\mu^{\beta\alpha}(k) e^{-ik\xi}}{s - S_\mu(k)} dk, \quad (1.14)$$

where P_μ are resolution of the identity projectors (of a finite matrix \hat{g}) and $S_\mu(k)$ are dispersion relation for ν bands (eigenvalues of \hat{g}). At the branch cut

$$\rho_{\xi;\mu}^{\beta\alpha}(\sigma) = \frac{1}{(2\pi)^d} \iint_{-\pi}^{\pi} P_\mu^{\beta\alpha}(k) \delta(\sigma + S_\mu(k)) e^{-ik\xi} dk. \quad (1.15)$$

Note that $S_\mu(k) < 0$ for all μ and k except for the edge band at $k = 0$ for which $S_1(0) = 0$.

1.4. Primitive lattices

For primitive lattices coordinates x can be identified with ξ , so that all formulas for ξ can be applied to x . In particular, $g_{yx} = g_{0, x-y} \equiv g_{x-y}$ since the coordinates are additive: if x and y are lattice sites then $x \pm y$ are also lattice sites. Each bond can be associated with a unit vector $\pm e^j$, $j = 1, \dots, \delta$, so that $w_0 = 2\delta$ with $\delta \geq d$. We number the bond vectors e^j in such a way that e^1, \dots, e^d are translation vectors, whereas e^{d+1}, \dots, e^δ are linear combinations of translation vectors with coefficients ± 1 . The band dispersion can be written explicitly:

$$S(k) = -w_0 + \sum_{|z|=1} \cos kz \equiv 2 \sum_{j=1}^{\delta} (\cos ke^j - 1). \quad (1.16)$$

The additive form of $S(k)$ allows to factorize the propagator. Indeed, let select the k -vectors in such a way that $ke^i = k_i$ for $i = 1, \dots, d$. Then

$$\hat{g}(t, k) = \prod_{i=1}^d e^{2t(\cos k_i - 1) - ik_i x_i} \prod_{j=d+1}^{\delta} e^{2t(\cos ke^j - 1)}.$$

For each ke^j we add a fictitious coordinate using the identity

$$f(ke^j) = \int_{-\pi}^{\pi} f(k'_j) \delta(k'_j - ke^j) dk'_j = \sum_{x'_j \in \mathbb{Z}} e^{ik'e^j x'_j} \frac{1}{2\pi} \int_{-\pi}^{\pi} f(k') e^{-ik'_j x'_j} dk'_j.$$

Therefore the propagator is fully factorized:

$$\tilde{g}_x(t) = e^{-w_0 t} \sum_{x'_{d+1}, \dots, x'_\delta \in \mathbb{Z}} \prod_{i=1}^d I_{x_i - z_i}(2t) \prod_{j=d+1}^{\delta} I_{x'_j}(2t), \quad z_i = \sum_{j=d+1}^{\delta} e_i^j x'_j, \quad (1.17)$$

where e_i^j is i -th lattice coordinate of j -th bond vector. Now it is easy to see that

$$g_x = \sum_{x' \in \mathbb{Z}^{\delta-d}} g_{x_1 - z_1, \dots, x_d - z_d, x'_{d+1}, \dots, x'_\delta}^{\text{hc}}, \quad (1.18)$$

where g^{hc} is the Green's function of the hypercubic lattice. In practice, there might exist a transformation of k -vectors such that the number of terms in Eq. (1.16) is minimized to minimize the number of summations in Eq. (1.17), especially for closed packed lattices for which the difference $\delta - d$ is large. Also there might be reduction to the Green's function of lattices other than hypercubic.

It is useful to introduce finite difference operators similar to the gradient in \mathbb{R}^d :

$$(\partial^j f)_x = f_{x+e^j} - f_x, \quad (\partial^{-j} f)_x = f_x - f_{x-e^j}, \quad \Delta^j = \partial^{-j} \partial^j, \quad D^j = \partial^{-j} + \partial^j \equiv f_{x+e^j} - f_{x-e^j},$$

so that $\Delta = \sum_j \Delta^j$. We will omit parentheses, writing $\partial^j f_x$ and so on. Some properties of these operators are described in Appendix 4.1. In this notations bond Green's function (1.5) can be written as

$$g_{(x, x+e^i)(y, y+e^j)} = \partial^i \partial^{-j} g_{x-y} = g_{x-y+e^i} + g_{x-y-e^j} - g_{x-y} - g_{x-y+e^i-e^j} \equiv \partial^j \partial^{-i} g_{y-x}.$$

For a primitive isotropic lattice, the function $G(x_1, \dots, x_\delta) = g_{x_1 e^1 + \dots + x_\delta e^\delta}$ is symmetric with respect to permutations of arguments and inversion. The ‘‘full symmetry’’ contain also other elements whose representation depends on the lattice type and choice of the coordinate system. Four classes of primitive isotropic lattices are considered here since they fully cover dimensions up to $d = 3$. The first is the hypercubic lattice \mathbb{Z}^d which is symmetric with respect to sign inversion at each coordinate independently. The second is body-centered hypercubic lattice \mathbb{I}_d which is primitive but is more convenient to describe in cubic coordinates. The 2^d nearest neighbors and the primitive translations are given by

$$e^{s_1 \dots s_d} = \sum_{j=1}^d s_j e^j / 2, \quad s_j = \pm 1, \quad e^i = \epsilon^i - \sum_{j=1}^d \epsilon^j / 2, \quad i = 1, \dots, d, \quad (1.19)$$

where ϵ^i are unit vectors of the cubic cell. The third is a face-centered hypercubic lattice corresponding to the \mathbb{D}_d root system. It is the sublattice of \mathbb{Z}^d with even $|x|$ so it is more convenient to describe it in the cubic cell. The $2d(d-1)$ nearest neighbors and the primitive translations are given by

$$e^{ij} = (\pm \epsilon^i \pm \epsilon^j) / 2, \quad 1 \leq i < j \leq d, \quad e^i = (\epsilon^i + \epsilon^{i+1}) / 2, \quad i = 1, \dots, d-1, \quad e^d = (\epsilon^d - (-1)^d \epsilon^1) / 2, \quad (1.20)$$

where the \pm signs are independent. The fourth is the symplectic honeycomb lattice of the root system \mathbb{A}_d . It is the hyperplane $\sum_{i=1}^{d+1} x_i = 0$ of \mathbb{Z}^{d+1} . The $d(d+1)$ nearest neighbors and the primitive translations are given by

$$e^{ij} = \epsilon^i - \epsilon^j, \quad 1 \leq i \neq j \leq d+1, \quad e^i = \epsilon^i - \epsilon^{d+1}, \quad i = 1, \dots, d. \quad (1.21)$$

1.5. Continual and large-scale approximations

At large scales Green's function of any lattice tends to the resolvent of Laplacian in \mathbb{R}^d which is [gfunRd]

$$g(s, x) = \frac{1}{(2\pi)^{d/2}} \left(\frac{\sqrt{s}}{\|x\|} \right)^{\frac{d}{2}-1} K_{\frac{d}{2}-1}(\sqrt{s}\|x\|). \quad (1.22)$$

In particular,

$$g_{d=1}(s, x) = \frac{e^{-\sqrt{s}\|x\|}}{2\sqrt{s}}, \quad g_{d=2}(s, x) = \frac{K_0(\sqrt{s}\|x\|)}{2\pi}, \quad g_{d=3}(s, x) = \frac{e^{-\sqrt{s}\|x\|}}{4\pi\|x\|}.$$

The inverse Laplace transformation of this function is the propagator of the diffusion equation [propRd]:

$$\tilde{g}(t, x) = \frac{1}{(4\pi t)^{d/2}} \exp\left(-\frac{\|x\|^2}{4t}\right), \quad (1.23)$$

which has maximum at $\|x\|^2 = 2dt$. The Fourier transforms have even simpler form:

$$\hat{g}(s, k) = \frac{1}{s + \|k\|^2}, \quad \hat{\tilde{g}}(t, k) = e^{-t\|k\|^2}.$$

To approximate a lattice Green's function by Eq. (1.23), the latter must be properly rescaled:

$$\tilde{g}^{\text{lat}}(t, x) = \frac{V_1}{(4\pi Dt)^{d/2}} \exp\left(-\frac{\|x\|^2}{4Dt}\right), \quad (1.24)$$

where V_1 is the volume per lattice point and $D = w_0/(2d)$ is the diffusion constant (both are unit for hypercubic lattice).

A more accurate description can be obtained within the large-scale approximation. It is easier to develop it for propagators and then perform the Laplace transformation of the result. The propagator of Eq. (1.14) is

$$\tilde{g}_{\xi; \mu}^{\beta\alpha}(t) = \frac{1}{(2\pi)^d} \int \int_{-\pi}^{\pi} P_{\mu}^{\beta\alpha}(k) e^{tS_{\mu}(k) - ik\xi} dk. \quad (1.25)$$

At large t and ξ this integral can be calculated by the saddle-point method. For simplicity we consider here primitive lattices with a generic dispersion, so that

$$\tilde{g}_x(t) = \frac{1}{(2\pi)^d} \int \int_{-\pi}^{\pi} e^{tS(k) - ikx} dk. \quad (1.26)$$

The saddle point of the exponent is at $k = -i\kappa$, where $\kappa \equiv \kappa(t)$ is a solution of the equations

$$\frac{\partial \tilde{S}}{\partial \kappa_i} = \frac{x_i}{t}, \quad i = 1, \dots, d, \quad \text{where } \tilde{S}(\kappa) = S(-i\kappa). \quad (1.27)$$

When the integration path in Eq. (1.26) is shifted by $-i\kappa$, the integrand has a sharp maximum at zero and reduced oscillations on the path, so that the integral can be approximated by the Gaussian one:

$$\tilde{g}_x(t) = \frac{1}{(2\pi)^d} \int \int_{-\pi}^{\pi} e^{tS(k-i\kappa) - \kappa x - ikx} dk \approx \frac{e^{t\tilde{S}(\kappa) - \kappa x}}{\sqrt{\det 2\pi t \tilde{S}''(\kappa)}}, \quad (1.28)$$

where \tilde{S}'' is the Hessian. If $t \rightarrow \infty$, $\kappa \rightarrow 0$ and $\tilde{S}(\kappa) \sim \kappa^2$ yielding $\kappa \sim x/t$ thus exactly recovering the continuum Green's function (1.24), provided that $\det \frac{\tilde{S}''(0)}{2D} = V_1^{-2}$.

The Laplace transformation of Eq. (1.28) can be performed only approximately by quadratic expansion of the exponent at the integrand's maximum (a variant of the saddle-point method) yielding:

$$g_x(s) \approx \sqrt{\frac{2\pi}{-\dot{\tilde{S}}}} \frac{e^{-\kappa x}}{\sqrt{\det 2\pi t \tilde{S}''}} \quad \text{with the equation } \tilde{S}(\kappa(t)) = s \text{ for } t, \quad (1.29)$$

where dot means time derivative, argument of \tilde{S} is omitted for clarity, and

$$-\dot{\tilde{S}} \equiv -\frac{\dot{\kappa}x}{t} \equiv t \sum_{i,j=1}^d \tilde{S}''_{ij} \dot{\kappa}_i \dot{\kappa}_j, \quad \text{so that } \dot{\kappa} = -\frac{(\tilde{S}'')^{-1}x}{t^2}. \quad (1.30)$$

For small s

$$t = \frac{\|x\|}{2\sqrt{s}} \implies g_x(s) \approx \frac{1}{2\sqrt{s}} \left(\frac{\sqrt{s}}{2\pi\|x\|}\right)^{\frac{d-1}{2}} e^{-\|x\|\sqrt{s}}. \quad (1.31)$$

Because of additional approximations made during the Laplace transformation, only the leading term of the continuum Green's function (1.22) is reproduced as $\|x\|\sqrt{s} \rightarrow \infty$. Nevertheless, numerical tests show that the large-scale approximation is accurate even for small x , see Fig. 12.

1.6. Path expansion

The Green's function of any graph can be calculated using the series

$$g(s) = \frac{1}{s+w} \sum_{n=0}^{\infty} \left(\frac{\Delta+w}{s+w} \right)^n = \frac{1}{s+w} \left(1 + \frac{\Delta+w}{s+w} \left(1 + \frac{\Delta+w}{s+w} (1 + \dots) \right) \right), \quad (1.32)$$

which is convergent for large enough s . Here w is a constant or a function of x . We will assume that $w \geq w_x$ so that all terms of the series are positive. If $w = w_x$ then Eq. (1.32) is the *path expansion* since $\Delta + w$ in this case contains only nondiagonal terms. In particular,

$$g_{xx}(s) = \frac{1}{(s+w_x)} + \sum_{z:|x-z|=1} \frac{t_{xz}t_{zx}}{(s+w_x)^2(s+w_z)} + \dots \quad (1.33)$$

where $t_{xz} = t_{zx} = 1$ for undirected bonds of unit strength. If w is a constant then Eq. (1.32) can be written explicitly as

$$g_{yx}(s) = \sum_{n=0}^{\infty} \frac{N_{yx}(n)}{(s+w)^{n+1+|x-y|}}, \quad (1.34)$$

where N_{yx} are integers for an integer w . If $w_x = w$ then $N_{yx}(n)$ is the number of paths of length $n + |x - y|$ between points x and y .

For a regular lattice, path expansion coefficients can be calculated from the Fourier integral (1.14):

$$g_{\xi}^{\beta\alpha}(s) = \sum_{n=0}^{\infty} \frac{N_{\xi}^{\beta\alpha}(n)}{(s+w)^{n+1+|\xi|}}, \quad N_{\xi}^{\beta\alpha}(n) = \frac{1}{(2\pi)^d} \iint_{-\pi}^{\pi} \sum_{\mu=1}^{\nu} P_{\mu}^{\beta\alpha}(k) (w + S_{\mu}(k))^{n+|\xi|} e^{-ik\xi} dk. \quad (1.35)$$

For many simple lattices, S_{μ} and $P_{\mu}^{\beta\alpha}$ are polynomials of e^{imk} -like terms (see e.g. Eq. (1.16)), and therefore by expansion of $P_{\mu}^{\beta\alpha} \cdot (w + S_{\mu})^{n'}$ the multidimensional integral (1.35) can be reduced to a multiple sum of products of one-dimensional trigonometric integrals which can be calculated using the formula

$$\frac{1}{\pi} \int_0^{\pi} (2 \cos k)^{2n+x} \cos kx dk = \binom{2n+x}{n}. \quad (1.36)$$

Evidently the best choice of the parameter w and the k -space basis is to minimize the number of terms in $w + S_{\mu}$ (see example of the triangular lattice below). Importantly, the products of one-dimensional integrals can usually be combined into path expansion coefficients of the lower-dimensional lattices, so that the multiple sum can be reduced to a single sum using the dimensional recursion (see e.g. Eq. (2.7)).

It is convenient to introduce the variable q and the function

$$h_x(q) = g_x(s(q)), \quad q = \frac{w}{s+w}, \quad s = w \frac{1-q}{q}, \quad (1.37)$$

because under proper choice of w , the path expansion coefficients are positive, the Green's function $h_x(q)$ is analytic for $|q| < 1$, has a singularity at $q = 1$, and is odd or even function of q for a bipartite lattice. In what follows we assume that w satisfies the above conditions. Now the series (1.35) can be written as

$$h_{\xi}^{\beta\alpha}(q) = \sum_{n=0}^{\infty} c_{\xi;n}^{\beta\alpha} q^{n+1+|\xi|}, \quad c_{\xi;n}^{\beta\alpha} = \frac{N_{\xi}^{\beta\alpha}(n)}{w^{n+1+|\xi|}}. \quad (1.38)$$

For large n and small S_{μ} , the power function in Eq. (1.35) can be approximated by the exponent $(w + S_{\mu})^{n'} \approx w^{n'} e^{tS_{\mu}}$, where $t = (n' + \varepsilon)/w$ and ε is a fitting parameter such that $\varepsilon = 0$ corresponds to the upper boundary. If $w > -\min_k S_{\mu}(k)$ then the maximum of $S_{\mu}(k)$ makes the dominant contribution to the Fourier integral. However, for some lattices the convenient choice of w might include k -points with $w = -\min_k S_{\mu}(k)$, so that their contributions should be taken into account too. Therefore,

$$c_{\xi;n}^{\beta\alpha} \approx \frac{\sigma_n}{w} \tilde{g}_{\xi}^{\beta\alpha} \left(\frac{n + \varepsilon + |\xi|}{w} \right), \quad (1.39)$$

where σ_n accounts for symmetry, e.g. for bipartite lattices if w is half-bandwidth then $\sigma_{2n} = 2$ and $\sigma_{2n+1} = 0$.

The fact that all terms of the series (1.38) are positive simplifies estimation of the series remainder

$$R_{\xi;n}^{\beta\alpha}(q) = \sum_{k=n}^{\infty} c_{\xi;k}^{\beta\alpha} q^{k+1+|\xi|} \quad (1.40)$$

for both error control and approximations. From Eq. (1.35) we can obtain Fourier integral representation

$$R_{\xi;n}^{\beta\alpha} = \frac{1}{(2\pi)^d} \iint_{-\pi}^{\pi} \sum_{\mu=1}^{\nu} P_{\mu}^{\beta\alpha}(k) \left(\frac{w + S_{\mu}(k)}{w + s} \right)^{n+|\xi|} \frac{e^{-ik\xi} dk}{s - S_{\mu}(k)}, \quad (1.41)$$

but it is unclear how to estimate it. Therefore, we approximate the series coefficients and then sum up the result. The estimate (1.39) is accurate but gives too complicated series even if the continuum propagator (1.24) is used. A possible workaround is to approximate the latter by a ‘‘summable’’ function:

$$\tilde{g}^{\text{lat}}(t, x) = \frac{V_1}{(4\pi Dt)^{d/2}} \exp\left(-\frac{\|x\|^2}{4Dt}\right) \lesssim V_1 \left(\frac{w}{4\pi D}\right)^{d/2} \left(wt + \frac{w}{2dD}\|x\|^2\right)^{-d/2} \quad (1.42)$$

resulting in

$$c_{\xi;n}^{\beta\alpha} \approx \frac{\sigma_n V_1}{w} \left(\frac{w}{4\pi D}\right)^{d/2} \left(n + \varepsilon + |\xi| + \frac{w}{2dD}\|\xi\|^2\right)^{-d/2}. \quad (1.43)$$

Now Eq. (1.40) can be summed up explicitly resulting in

$$R_{\xi;n}^{\beta\alpha}(q) \approx R_{\xi;n}^{\Phi}(q, \varepsilon) \quad (1.44)$$

where ε is a parameter and functional form of R^{Φ} depends on σ_n :

$$R_{\xi;n}^{\Phi}(q, \varepsilon) = \frac{V_1}{w} \left(\frac{w}{4\pi D}\right)^{d/2} q^{n+1+|\xi|} \Phi\left(q, \frac{d}{2}, n + \varepsilon + |\xi| + \frac{w}{2dD}\|\xi\|^2\right), \quad \text{for } \sigma_n = 1, \quad (1.45a)$$

$$R_{\xi;2n}^{\Phi}(q, \varepsilon) = \frac{2V_1}{w} \left(\frac{w}{8\pi D}\right)^{d/2} q^{2n+1+|\xi|} \Phi\left(q^2, \frac{d}{2}, n + \frac{1}{2}(\varepsilon + |\xi| + \frac{w}{2dD}\|\xi\|^2)\right), \quad \text{for } \sigma_{2n} = 2, \sigma_{2n+1} = 0, \quad (1.45b)$$

where Φ is the Lerch transcendent function. According to Eq. (1.42), these approximations are accurate if

$$n + |\xi| \gg \frac{w}{2dD}\|\xi\|^2, \quad (1.46)$$

otherwise they provide only the upper boundary. The best estimate is expected for the value of ε corresponding to the large- n asymptotics of the path expansion coefficients, which we denote by ε_{∞} . Then the strict upper boundary can be obtained with $\varepsilon_{\text{up}} \leq \varepsilon_{\infty}$. A tight lower boundary in the functional form of Eq. (1.43) is meaningful only for small ξ with some $\varepsilon_{\text{low}} > \varepsilon_{\infty}$, see Figs. 7 and 8. In a general case, the lower boundary is zero. Values of the discussed above parameters for some lattices are listed in Table 1

Table 1: Values parameters used in Eqs. (1.43) and (1.45) for some lattices. The ε_{up} is determined by numeric test for path expansion coefficients.

Lattice	σ_n	V_1	D	ε_{∞}	ε_{up}
hypercubic	2/0	1	1	1/2	$1/4^{d \leq 6}$
triangular	1	$\sqrt{3}/2$	3/2	1/3	1/3

By taking $n = 0$ in Eq. (1.45) we obtain the approximation to Green's function itself:

$$h_x(q) \approx R_{x;0}^{\Phi}(q, \varepsilon), \quad (1.47)$$

where ε should be determined by some fitting procedure. The simplest fitting is by the first path expansion coefficient yielding accurate approximation for the Green's function at origin, see Fig. 3. See other examples in Fig. 4.

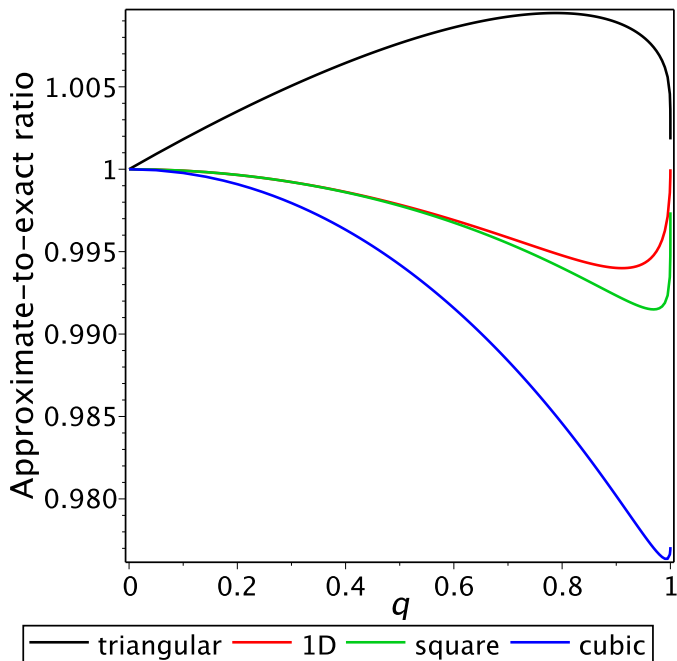


Figure 3: Lerch transcendent approximation to Green's function of several lattices at origin. Here ε is determined by the first path expansion coefficient (e.g. $\varepsilon = 2^{2/d}/2\pi$ for hypercubic lattices).

1.7. Recurrence formulas and series at singularities

The Laplace equation itself cannot provide a platform for recurrent evaluation of the Green's function in multiple dimensions. However, there is a hidden space-time symmetry due to the translational invariance which can provide additional identities enough to derive one-dimensional recurrence relations. For simplicity we consider primitive lattices but discussed ideas can be applied to any lattice with a root-free dispersion $S(k)$. By differentiating the Fourier transform of the propagator $\hat{g}(t, k) = e^{tS(k)}$ with respect to k_i and then taking the inverse Fourier transform, we get d identities for the propagator:

$$-\frac{t}{x_i} \sum_{|z|=1} z_i \tilde{g}_{x+z}(t) = \tilde{g}_x(t), \quad i = 1, \dots, d, \quad (1.48)$$

or equivalent identities for the Green's function and its integral:

$$\frac{1}{x_i} \sum_{|z|=1} z_i g_{x+z}(s) = - \int_s^\infty g_x(s') ds', \quad i = 1, \dots, d, \quad (1.49)$$

where it is assumed that $x_i \neq 0$. Note that the sum can be written in terms of the bond vectors:

$$\sum_{|z|=1} z_i f_{x+z} \equiv \sum_{j=1}^{\delta} e_i^j D^j f_x. \quad (1.50)$$

Importantly, the right-hand side of Eq. (1.49) does not depend on i , so that we have $d - 1$ identities for the Green's function itself:

$$\frac{1}{x_i} \sum_{|z|=1} z_i g_{x+z}(s) = \text{const}(i), \quad i = 1, \dots, d. \quad (1.51)$$

Combined with the Laplace equation they provide the required recurrence relations at least for lattices with low enough coordination number. The easiest recursion is to resolve g_x plane-by-plane from a given point to the origin. It requires existence of a plane whose lattice points have no more than d nearest neighbors at

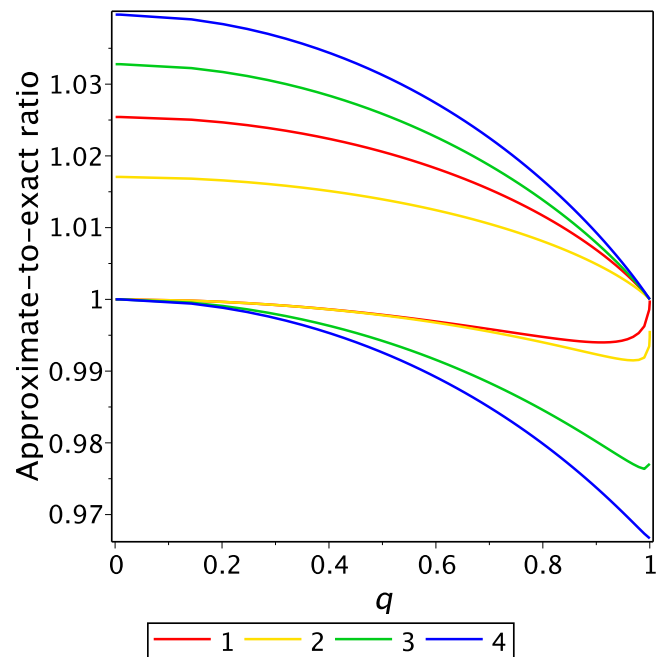


Figure 4: Error of approximation of the hypercubic Green's function at origin by Lerch transcendent. Different colors correspond to dimensions 1 to 4. The lower and upper boundaries are obtained by fitting values at $q = 0$ and $q = 1$.

one side out of the plane. For hypercubic lattices any plane satisfies this condition. For symplectic honeycomb lattice \mathbb{A}_d , including triangular and face-centered cubic lattices, the condition is satisfied by \mathbb{A}_{d-1} plane which is $(11 \dots 1)$ plane in the coordinate system (1.21). For the body-centered cubic lattice the required plane is (110) . The computing path of such recurrences can be determined iteratively by recursive evaluations or optimized to achieve a better linear scaling with distance. Usually such a path has two parts: the first is to the nearest high-symmetry point and then along the high-symmetry direction. The recurrence propagates differences thus requiring high-precision evaluations at large s . It should be noted that known recurrence schemes in two-dimensional [Morita71b] and three-dimensional [Joyce02] cases are different from the proposed scheme but can be derived from it.

Because Eq. (1.51) includes only nearest neighbors, the recurrence basis includes only the origin and its symmetry-unique neighbors. For primitive isotropic lattices we can write the basis explicitly:

$$g_x = \sum_{n=0}^d P_n g_n, \quad g_n = g_{e^1+e^2+\dots+e^n}, \quad (1.52)$$

where P_n are polynomials in $s + w_0$ (or $1/q$) and g_n constitute a ‘‘basis’’: values of the Green's function at the seeding core of the recurrence equation. Here we assume that vectors e^i are chosen in such a way that all points $e^1 + e^2 + \dots + e^n$ are inequivalent by symmetry. The basis size is $d + 1$ because vectors e^1, \dots, e^d taken with unit coefficients span all points within one unit cell distance from the origin, whereas all other points are reducible to them by Eq. (1.52).

By differentiating Eq. (1.49) we obtain

$$\frac{1}{x_i} \sum_{|z|=1} z_i g'_{x+z} = g_x, \quad (1.53)$$

which together with Eq. (1.52) to exclude non-basis functions will produce a set of $d + 1$ first-order linear differential equations for g_0, \dots, g_d with the coefficients linear in s . This set is equivalent to a d -order linear differential equation for g_0 with polynomial coefficients in s or q . The reduced order is caused by the algebraic relation between g_0 and g_1 (for an isotropic lattice):

$$w_0 g_1 = (s + w_0) g_0 - 1. \quad (1.54)$$

For example, in one dimension we have

$$\begin{cases} (s+2)g'_1 = 2g'_0, \\ 2g_1 = (s+2)g_0 - 1, \end{cases} \implies s(s+4)g'_0 + (s+2)g_0 = 0 \quad \text{or} \quad q(1-q^2)h'_0 - h_0 = 0.$$

These equations can be used in particular for performing series expansion at singularities since alternative approaches are challenging [Joyce03a].

1.8. Evaluation of lattice Green's functions

Besides the one-dimensional case the evaluation of lattice Green's functions is nontrivial. Available methods can be summarized as follows (see also Fig. 1):

- Fourier integrals (1.14) are the most universal since they provide a solution for any lattice at any values of arguments. However, they are computationally inefficient at singularities and large x , requiring ultrafine k -grids and use of arbitrary-precision arithmetic for large x , see Table 2. Note that the dimension of the integral can be reduced if a lower-dimensional Green's function is known.
- Path expansion (1.34) is very efficient for $\Re s \geq 0$ if its coefficients are known. Since all summands are positive, one can get also the error bar. For the hypercubic lattice the computational bottleneck in Maple is the evaluation of the Lerch transcendent function providing the estimate of the series remainder.
- If outward recurrence relations are known, it is enough to calculate the Green's function at several points near the origin and then use the recurrence to evaluate its value at other points. It is especially useful because for all simple 2D and 3D lattices, $g_0(s)$ can be represented in terms of known special functions. However, for large x use of arbitrary-precision arithmetic is required to prevent the precision loss.

- If propagator is known, Laplace integrals (2.3) can be used by they are not efficient for computations.
- Large-scale approximation (up to the continuum approximation (1.22)) is useful for large x but has finite precision.

Table 2: Benchmarking path expansion series and Fourier integral for evaluation of the Green's function of the simple cubic lattice. Here 'series' means Eq. (1.34) with the remainder estimated by Eq. (1.45a), 'sum' means the series without remainder, and 'Fourier' means Eq. (1.14) with half-shifted uniform k-grid. Question marks denote hardly computable cases. Also, at large distances the remainder Eq. (1.45a) is not precise. Single precision means relative error below 10^{-8} . The asterisk * indicates insufficiency of double-precision calculations.

s	Parameters		Exact value	Number of terms		
	(x, y, z)	precision		series	sum	Fourier
1	(0,0,0)	single	0.170523807	0	40	100
1	(8,6,3)	single	$2.3 \cdot 10^{-7}$	–	70	1000
1	(80,60,30)	single	$2.0 \cdot 10^{-48}$	–	200	10^{5*}
0	(0,0,0)	1%	0.252731010	1	1000	4000
0	(0,0,0)	0.1%		100	?	$4 \cdot 10^6$
0	(0,0,0)	single		100	?	?

§2. Hypercubic lattice

2.1. General statements

For convenience we will use three different arguments of the Green's function:

$$g_x(s) = \mathcal{G}_x(\omega) = h_x(q), \quad s + 2d = \omega = 2d/q, \quad (s + 2d) \frac{dg}{ds} = \omega \frac{d\mathcal{G}}{d\omega} = -q \frac{dh}{dq}. \quad (2.1)$$

In the literature another function is sometimes used: $\mathcal{G}_x^{\text{Joyce}}(\omega^{\text{Joyce}}) = 2\mathcal{G}_x(\omega)$ with $2\omega^{\text{Joyce}} = \omega$. The hypercubic lattice is primitive, $\delta = d$, $|x| = |x_1| + \dots + |x_d|$ [latDscCD], and $\|x\|^2 = x_1^2 + \dots + x_d^2$ [latDscED2], see also Fig. 5. The dispersion is $S(k) = -2d + 2 \sum_{i=1}^d \cos k_i$, and the optimal k-grid is shifted by $\lambda = 1/2$ allowing to calculate g at singularities. The propagator is factorized [latDscp]:

$$\tilde{g}_x(t) = e^{-2dt} \prod_{i=1}^d I_{x_i}(2t) \quad (2.2)$$

allowing for another integral representation of Green's function [latDscgI]:

$$g_x(s) = \int_0^\infty e^{-st-2dt} I_{x_1}(2t) \dots I_{x_d}(2t) dt. \quad (2.3)$$

This integral diverges for $\Re s < 0$, therefore another one is used converging for $\Im s > 0$ [latDscgI.alt]:

$$g_x(s) = i^{-1-x_1-\dots-x_d} \int_0^\infty e^{i(s+2d)\tau} J_{x_1}(2\tau) \dots J_{x_d}(2\tau) d\tau. \quad (2.4)$$

The function $\mathcal{G}(\omega)$ is odd or even according to Eq. (1.3), thus it is sufficient to consider $\omega \geq 0$. It is analytical function with branch cut $[-2d, 2d]$ and singularities at the points: $\omega = -2d, -2d + 4, \dots, 2d - 4, 2d$ (or $s = -4d, \dots, -4, 0$). At infinity it has a simple pole: $\mathcal{G}(\omega) = 1/\omega + 2d/\omega^3 + \dots$. In terms of Fourier integrals, \mathcal{G} can be evaluated recurrently in d with the use of the identity

$$\mathcal{G}(\omega; x_1, \dots, x_d) = \frac{1}{\pi} \int_0^\pi \mathcal{G}(\omega - 2 \cos k_d; x_1, \dots, x_{d-1}) \cos k_d x_d dk_d.$$

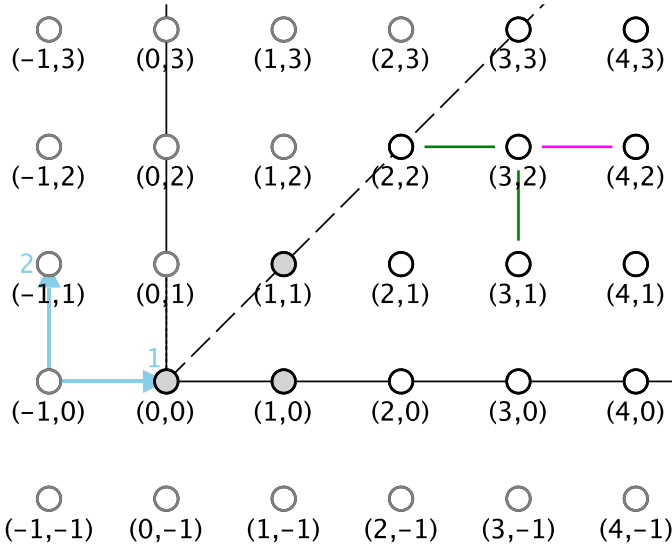


Figure 5: Square lattice coordinate system and notations. Cartesian vectors corresponding to k_1 and k_2 are shown as blue arrows. Recurrence scheme for evaluation of $g_{(4,2)}$ is shown by colored bonds.

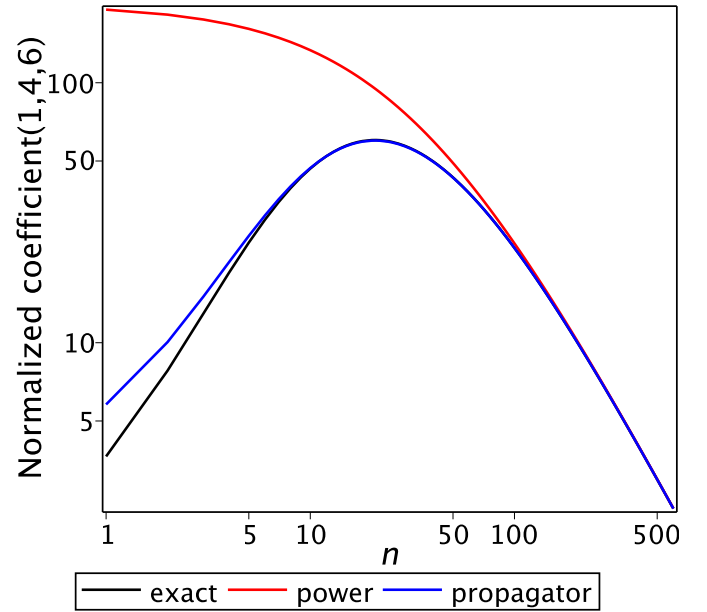


Figure 6: Two approximations of path expansion coefficients for simple cubic lattice.

As a function of spatial coordinates, $g(s; x_1, \dots, x_d)$ is symmetric with respect to any permutation of arguments and any inversion of their signs, so that it is sufficient to consider the fundamental domain $x_1 \geq x_2 \geq \dots \geq x_d \geq 0$ [latDscX]. When summing up the symmetric function over the lattice it is necessary to know the orbits [latDsc0] of the symmetry group and their sizes [latDscONT]. Let us denote the permutation group by S_d and the symmetry group of the hypercubic lattice by S'_d . Orbits of S'_d can be enumerated by incomplete ordered partitions of the integer d as follows. For any partition $P = \{d_1, \dots, d_k\}$, $d_1 > \dots > d_k > 0$ the corresponding orbit contains points

$$\left(\underbrace{0, \dots, 0}_{d_0}, \underbrace{x_1, \dots, x_1}_{d_1}, \dots, \underbrace{x_k, \dots, x_k}_{d_k} \right),$$

where $d_0 = d - d_1 - \dots - d_k$ and x_1, \dots, x_k are distinct nonzero numbers. The stabilizer of this orbit is $S_{d_1} \otimes \dots \otimes S_{d_k} \otimes S'_{d_0}$, hence the orbit size

$$|P| = 2^{d-d_0} \binom{d}{d_0, d_1, \dots, d_k}.$$

2.2. Path expansion

Here we assume that $x_i \geq 0$. Coefficients $N_x(n) \equiv N_{0x}(n)$ in the series (1.34) can be obtained from Eq. (2.3) [latDscN]:

$$N_x(2n) = \sum_{n_i \geq 0}^{\sum_i n_i = n} \binom{2n + |x|}{n_1, n_1 + x_1, \dots, n_d, n_d + x_d}, \quad N_x(2n+1) = 0, \quad (2.5)$$

where the expression in the parentheses denote multinomial coefficients. The leading term of the expansion is

$$g_x(s) \sim \binom{|x|}{x_1, \dots, x_d} \frac{1}{(s + 2d)^{1+|x|}}. \quad (2.6)$$

The sum (2.5) can be evaluated recursively in d [Maassarani00]:

$$N_x(2n) = \sum_{k=0}^n N_{(x_1, \dots, x_m)}(2k) \binom{2n + |x|}{2k + x_1 + \dots + x_m} N_{(x_{m+1}, \dots, x_d)}(2n - 2k) \quad (2.7)$$

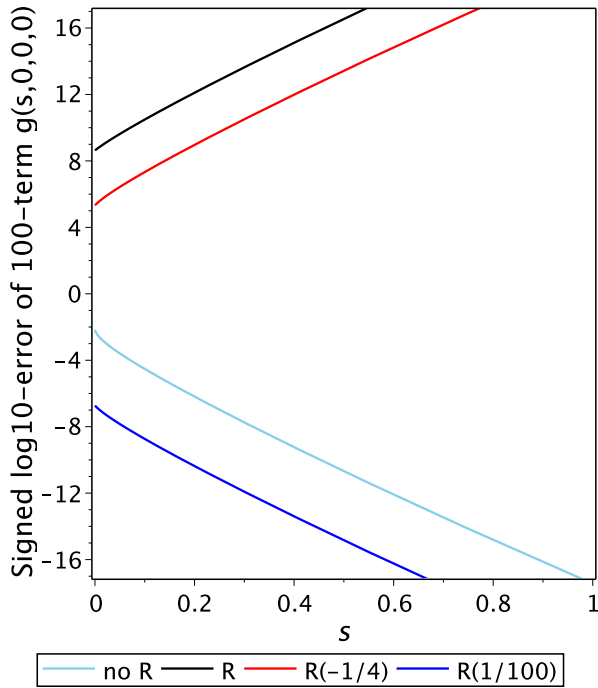


Figure 7: Error in evaluation of the Green's function of the simple cubic lattice at origin by path expansion with different $\epsilon_{\text{up,low}} - \epsilon_{\infty}$ (shown in parentheses) in the remainder (1.45b).

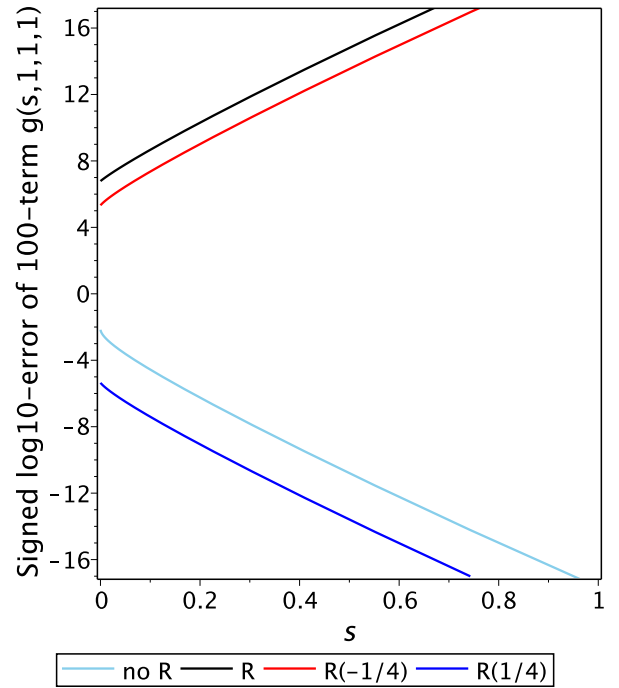


Figure 8: The same as in Fig. 7 but at the lattice point $(1, 1, 1)$ and with different ϵ_{low} .

starting with explicit formulas for $d = 1, 2$:

$$N_{(x)}(2n) = \binom{2n+x}{n}, \quad N_{(x,y)}(2n) = \binom{2n+x+y}{n} \binom{2n+x+y}{n+x}. \quad (2.8)$$

2.3. Recurrence relations and series at $s = 0$

For hypercubic lattice Eq. (1.51) reduces to

$$\frac{1}{x_i} D^i g_x = \text{const}(i), \quad i = 1, \dots, d, \quad (2.9)$$

yielding the recurrence:

$$g_{x+e^1} = g_{x-e^1} + \frac{x_1}{|x|} \left((s+2d)g_x - 2 \sum_{i=1}^d g_{x-e^i} \right). \quad (2.10)$$

The expansion coefficients P_n in Eq. (1.52) are polynomials in $s+2d$ of the degree $\max_i |x_i| - 1$. The same recursion can be applied to path expansion coefficients yielding

$$N_{x+e^1}(2(n-1)) = N_{x-e^1}(2n) + \frac{x_1}{|x|} \left(N_x(2n) - 2 \sum_{i=1}^d N_{x-e^i}(2n) \right). \quad (2.11)$$

The recurrence basis of Eq. (1.52) is shown in Fig. 9 in terms of $h_n(q)$. To obtain the differential equation for the basis functions, we combine Eq. (2.9) written for e^n

$$g'_{n+e^n} - g'_{n-1} = g_n$$

with the Laplace equation centered at g_n

$$(s+2d)g_n = n(g_{n+e^n} + g_{n-1}) + 2(d-n)g_{n+1},$$

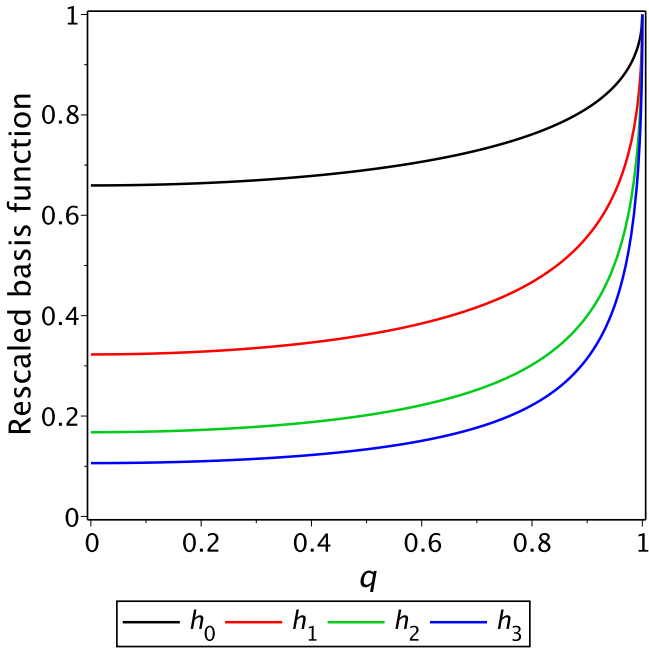


Figure 9: Recurrence basis for the simple cubic lattice. The functions are rescaled as $h_n(q)/h_n(1)/q^{n+1}$.

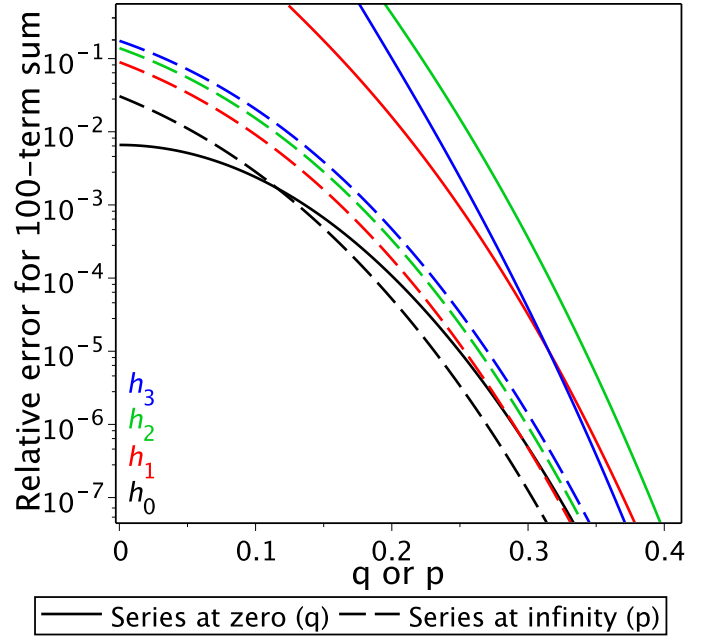


Figure 10: Error in evaluation of h_n functions for simple cubic lattice by two kinds of series near their convergence boundary.

where $n + e^n \equiv e^1 + \dots + e^{n-1} + 2e^n$. By excluding g_{n+e^n} , we arrive to the set of equations for $g_n(s)$

$$(s + 2d)g'_n - 2ng'_{n-1} - 2(d-n)g'_{n+1} = (n-1)g_n \quad (2.12)$$

or equivalent set for $h(q)$

$$h'_n - (n/d)qh'_{n-1} - (1-n/d)qh'_{n+1} = (1-n)q^{-1}h_n \iff dq^{-n}(q^{n-1}h_n)' = nh'_{n-1} + (d-n)h'_{n+1}. \quad (2.13)$$

The determinant of the tridiagonal matrix at h' is equal to $Q(q)/Q(0)$, where

$$Q(q) = \prod_{k=0}^{[(d-1)/2]} (q^2 - q_k^2), \text{ and } q_k = \frac{d}{d-2k} \quad (2.14)$$

are singularities of the Green's function. The set of first-order equations (2.13) can be converted to a single high-order equation for h_0 :

$$\sum_{n=0}^d Q_n(q) \left(q \frac{d}{dq} \right)^n h_0(q) = 0, \quad Q_d = Q, \quad Q_{d-1} = dq^4 \frac{d}{dq^2} \frac{Q(q)}{q^2}, \quad Q_0 = (-1)^d Q(0), \quad (2.15)$$

and the rest of Q_n are polynomials of q^2 of the same order as Q . The conversion matrix from derivatives $\{h'_0, h''_0, \dots, h_0^{(d)}\}$ to set $\{h_0, h_2, h_3, \dots, h_d\}$ is polynomial in q divided by some power of q . Notice absence of h_1 in this set, which relates to h_0 via Eq. (1.54). Such conversion allows to replace the basis $\{g_0, g_{e^1}, g_{e^1+e^2}, \dots, g_{e^1+e^2+\dots+e^d}\}$ in Eq. (1.52) by $\{g_0, g'_0, \dots, g_0^{(d-1)}, 1\}$ which includes only g_0 and its derivatives.

All solutions of Eq. (2.13) can be obtained as series in the variable $z = 1 - q^2$ or $p = \sqrt{z}$:

$$q^{n-1}h_n(q) = A_n(p^2) + Z(p)B_n(p^2), \quad Z(p) = p^{d-2} \begin{cases} 1 & \text{for odd } d, \\ \ln(p_0/p) & \text{for even } d, \end{cases} \quad (2.16)$$

where $A(z)$ and $B(z)$ are analytic functions for $|z| < 1$ and p_0 is a free parameter which is convenient to set to $p_0 = 4$ for $d = 2$ and $p_0 = 1$ otherwise. If we constrain h_1 by Eq. (1.54), then Eq. (2.13) will have d linear

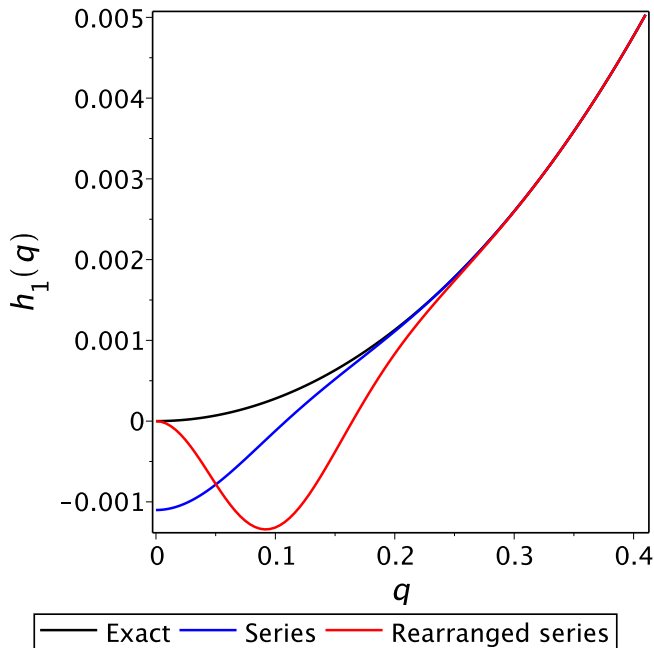


Figure 11: Convergence of $s = 0$ series at $q = 0$. Here the rearrangement is aimed to get the correct asymptotics at $q = 0$, but that increases the error for nonzero q .

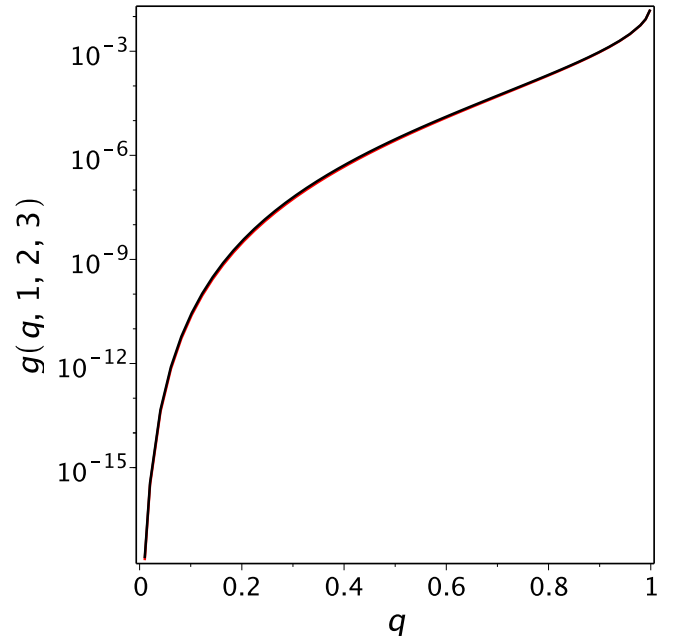


Figure 12: Large-scale approximation for simple cubic lattice is accurate even for small values of coordinates.

independent solutions: $d - 1$ regular ($B = 0$) and one singular ($B \neq 0$). The Green's function (2.16) can now be written as

$$q^{n-1}h_n(q) = \sum_{m=1}^d C_m A_{mn}(p^2) + C_d Z(p) B_{dn}(p^2) + \delta_{n1} \left(C_1 - \frac{1}{2d} \right), \quad (2.17)$$

where regular solutions are labeled as A_{mn} with $m = 0, \dots, d-2$ and the singular one is labeled as A_{dn} and B_{dn} , so that index m enumerates the differential equation basis and n enumerates the recurrence basis. Here A_{mn} are defined as solutions of Eq. (2.13) with $A_{m0}(z) = z^m + o(z^{d-2})$, whereas the singular solution is obtained under the conditions $B_{dn}(0) = 1$ and $A_{d0} = o(z^{d-2})$. Series for all $A_{mn}(z)$ and $B_{dn}(z)$ have rational coefficients which can be determined recursively using Eq. (2.13). The coefficient at the singular part is given by [Joyce03a]

$$C_d = (-1)^{\lfloor \frac{d-1}{2} \rfloor} \frac{1}{2^d \Gamma(d/2)} \left(\frac{d}{\pi} \right)^{d/2-1} \begin{cases} 1 & \text{for odd } d, \\ 2/\pi & \text{for even } d. \end{cases} \quad (2.18)$$

Coefficients at regular solutions are zero in lower dimensions and nontrivial in higher dimensions, e.g., for $d = 3$

$$C_1 = h_0(1), \quad C_2 = \frac{9h_0(1)}{32} + \frac{3}{64\pi^2 h_0(1)}.$$

Technical details are given in Section 4.5. Accuracy of the series is shown in Fig. 10: it is decreasing with distance from the origin faster than for path expansion series. Details of that inaccuracy are shown in Fig. 11.

2.4. Large-scale approximation

Here we assume that $x_i \geq 0$. Since the propagator is factorized for the hypercubic lattice, it is sufficient to consider the one-dimensional case. We have $\tilde{S} = 2(\cosh \kappa - 1)$, and Eq. (1.27) can be solved explicitly reproducing the uniform approximation of the Bessel functions:

$$\tilde{g}_x(t) \approx \frac{\exp[2t(\cosh \kappa - 1 - \kappa \sinh \kappa)]}{\sqrt{2\pi t \cosh \kappa}}, \quad \sinh \kappa = \frac{x}{2t}. \quad (2.19)$$

For the Green's function, Eq. (1.29) reduces to [latDscgL]

$$g_x(s) \approx Q_x(s) \equiv \frac{1}{2} (4\pi t)^{\frac{1-d}{2}} \left(\prod_{i=1}^d \cosh \kappa_i \cdot \sum_{i=1}^d \frac{\sinh^2 \kappa_i}{\cosh \kappa_i} \right)^{-1/2} \exp \left(- \sum_{i=1}^d \kappa_i x_i \right), \quad \sinh \kappa_i = \frac{x_i}{2t}, \quad (2.20)$$

where the equation for t transforms to

$$\sum_{i=1}^d \left(\sqrt{1 + \frac{x_i^2}{4t^2}} - 1 \right) = \frac{s}{2}. \quad (2.21)$$

Note that

$$\frac{\max_i x_i}{\sqrt{s(4+s)}} \leq t \leq \frac{\max_i x_i}{\sqrt{\frac{s}{d}(4+\frac{s}{d})}} \equiv \frac{q \max_i x_i}{2p},$$

where the left equality is reached when all x_i are equal and the right equality is reached when all but one x_i are zero. For large s , $|x|/t \approx s + 2d$ and $e^{\kappa_i} \approx x_i/t$ are large, and Q approximates the leading term (2.6):

$$Q_x(s) \approx (2\pi)^{\frac{1-d}{2}} \frac{|x|^{|x|+1/2}}{\prod_{i=1}^d x_i^{x_i+1/2}} \frac{1}{(s+2d)^{1+|x|}}.$$

Alternatively, we can approximate the sum (1.34) together with the nested sums (2.5) by an integral and use Stirling's formula to approximate factorials:

$$g_x(s) \approx \frac{1}{s+2d} \int_n \sqrt{\frac{2\pi(2n+|x|)}{\prod_{i=1}^d 4\pi^2 n_i(n_i+x_i)}} e^{S(n_1, \dots, n_d)} dn_1 \dots dn_d,$$

where

$$S(n_1, \dots, n_d) = (2n+|x|) \ln(2n+|x|) - \sum_{i=1}^d [n_i \ln n_i + (n_i+x_i) \ln(n_i+x_i) + (2n_i+x_i) \ln(s+2d)].$$

Now we will use Laplace's method to evaluate the integral. The extremum of S is reached at n_i satisfying the equation $n_i(n_i+x_i) = t^{-2}$, where $t = \frac{2n+|x|}{s+2d}$ (we will use the same notations for integrating variables and the their values at the extremum). The equation for this t coincides with Eq. (2.21). The Hessian is

$$\frac{\partial^2 S}{\partial x_i \partial x_j} = \frac{4}{2n+|x|} - \delta_{ij} \frac{2n_i+x_i}{n_i(n_i+x_i)} \equiv \frac{2}{t} \left(\frac{1}{d+s/2} - \delta_{ij} \cosh \kappa_i \right),$$

so that

$$\det(-S'') = \left[\sum_{i=1}^d \frac{4n_i(n_i+x_i)}{(2n+x)(2n_i+x_i)} - 1 \right] \prod_{i=1}^d \frac{2n_i+x_i}{n_i(n_i+x_i)},$$

and we arrive to Eq. (2.20). The eigenvalues of the Hessian satisfy the equation

$$\sum_{i=1}^d \frac{1}{\lambda t/2 + \cosh \kappa_i} = d + s/2.$$

We see that at large s the eigenvalues are large: $\lambda_i \approx -x_i/t^2$, whereas at small s they are small and isotropic: $\lambda \approx -2s/dt$, thus clarifying the limited accuracy of Eq. (2.20) at small s .

2.5. Periodic hypercubic lattice

For periodic lattice dispersion relation is the same as for infinite lattice so that Fourier integrals are simply replaced by sums:

$$g_x(s) = \frac{1}{V} \sum_k \frac{e^{-ikx}}{s + 2 \sum_{i=1}^d (1 - \cos k_i)}, \quad k_i = \frac{2\pi l_i}{L_i}, \quad l_i = \overline{0, L_i - 1}.$$

Note the evaluation formula

$$\begin{aligned}
g(s; x_1, \dots, x_d) &= \frac{1}{L_d} \sum_{k_d} e^{-ik_d x_d} g(s + 2[1 - \cos k]; x_1, \dots, x_{d-1}) \\
&= \frac{g(s; x_1, \dots, x_{d-1})}{L_d} + \frac{2}{L_d} \sum_{l=1}^{\lfloor \frac{L_d-1}{2} \rfloor} \cos\left(\frac{2\pi l x_d}{L_d}\right) g\left(s + 2\left[1 - \cos \frac{2\pi l}{L_d}\right]; x_1, \dots, x_{d-1}\right) \\
&\quad + \mathcal{I}\{L_d \text{ is odd}\} \frac{(-1)^{x_d} g(s + 4; x_1, \dots, x_{d-1})}{L_d}.
\end{aligned}$$

If $L_1 = L_2 = \dots = L$ then the mean square displacement

$$\begin{aligned}
\langle \delta x^2 \rangle &= \sum_x (x_1^2 + \dots + x_d^2) g_x(s) = \frac{2d}{s^2} + \frac{dL^2}{2s} - \frac{dL^2}{2} \left(1 + \frac{4}{sL}\right) g_0(s) \\
&= \frac{d(L-1)(2L-1)}{6s} + \frac{(L^2-1)(L^2-15L+11)}{360} + O(s).
\end{aligned}$$

In the time domain we have the similar to (2.2) expression:

$$g_x(t) = e^{-2dt} \prod_{i=1}^d I_{x_i, L_i}(2t),$$

where

$$I_{x,L}(2t) = \frac{1}{L} \sum_{l=0}^{L-1} \exp\left[2t \cos\left(\frac{2\pi l}{L}\right) - i\frac{2\pi l}{L}x\right] \equiv \frac{e^{2t}}{L} + \frac{2}{L} \sum_{l=1}^{\lfloor \frac{L-1}{2} \rfloor} e^{2t \cos \frac{2\pi l}{L}} \cos\left(\frac{2\pi l x}{L}\right) + \mathcal{I}\{L \text{ is odd}\} \frac{(-1)^x e^{-2t}}{L}.$$

2.6. Square lattice

The natural basis is

$$h_0 = \frac{q\mathcal{K}}{4}, \quad h_1 = \frac{\mathcal{K}-1}{4}, \quad h_2 = \frac{(2-q^2)\mathcal{K}-2\mathcal{E}}{4q}, \quad \text{where } \mathcal{K} = \frac{2}{\pi}K(q), \quad \mathcal{E} = \frac{2}{\pi}E(q). \quad (2.22)$$

At $q = 1$ Green's function diverges but the function $\delta g_{xy} = g_{xy} - g_{00}$ is finite. It can be calculated by use of the same recurrence relations as for g , starting from $\delta g_{00} = 0$, $\delta g_{10} = -1/4$, and $\delta g_{11} = -1/\pi$. In particular,

$$\delta g_{xx} = \frac{1}{2\pi} \left[\psi\left(\frac{1}{2}\right) - \psi\left(x + \frac{1}{2}\right) \right].$$

The density of states is given by

$$\rho(\sigma) = \frac{1}{2\pi^2} K\left(\frac{\sqrt{\sigma(8-\sigma)}}{4}\right), \quad 0 \leq \sigma \leq 8. \quad (2.23)$$

Path expansion series are hypergeometric:

$$h_{xy}(q) = \left(\frac{q}{4}\right)^{x+y+1} \frac{(x+y)!}{x!y!} {}_4F_3\left(\frac{x+y+1}{2}, \frac{x+y+1}{2}, \frac{x+y+2}{2}, \frac{x+y+2}{2}; x+1, y+1, x+y+1; q^2\right)$$

and can be calculated recurrently:

$$h_{xy}(q) = \sum_{n=0}^{\infty} a_n, \quad a_n = a_{n-1} \frac{[(2n+x+y)(2n-1+x+y)]^2}{n(n+x)(n+y)(n+x+y)} \left(\frac{q}{4}\right)^2, \quad a_0 = \frac{(x+y)!}{x!y!} \left(\frac{q}{4}\right)^{x+y+1}.$$

Symmetry reduction works as follows:

$$\begin{aligned} \sum_{x,y=-L}^L \varphi(g_{xy}) &= \varphi(g_{00}) + 4 \sum_{x=1}^L \varphi(g_{x0}) + 4 \sum_{x=1}^L \varphi(g_{xx}) + 8 \sum_{x=2}^L \sum_{y=1}^{x-1} \varphi(g_{xy}) \quad [\text{lat2sqadd}], \\ \sum_{x,y=-L}^L \varphi(\Delta^1 g_{xy}) &= \varphi(\Delta^1 g_{00}) + 2 \sum_{x=1}^L \varphi(\Delta^1 g_{x0}) + 2 \sum_{y=1}^L \varphi(\Delta^1 g_{0y}) + 4 \sum_{x,y=1}^L \varphi(\Delta^1 g_{xy}), \\ \sum_{x=-L}^{L-1} \sum_{y=1-L}^L \varphi(\partial^1 \partial^{-2} g_{xy}) &= 2 \sum_{x=0}^{L-1} [\varphi(\partial^1 \partial^{-2} g_{x,x+1}) + \varphi(-\partial^1 \partial^{-2} g_{x,x+1})] \\ &\quad + 4 \sum_{x=1}^{L-1} \sum_{y=1}^x [\varphi(\partial^1 \partial^{-2} g_{xy}) + \varphi(-\partial^1 \partial^{-2} g_{xy})]. \end{aligned}$$

Evaluation of Green's function at any point can be performed by the alternative recurrence scheme described in Ref. [Morita71]. Starting from g_{00} and g_{11} we calculate the diagonal elements by the relation

$$g(x+1, x+1) = \frac{4x}{2x+1} (2q^{-2} - 1)g(x, x) - \frac{2x-1}{2x+1} g(x-1, x-1), \quad x \geq 2.$$

Then the rest of the points can be calculated recursively column by column:

$$g(1, 0) = q^{-1}g(0, 0) - \frac{1}{4},$$

and for all the subsequent columns:

$$\begin{aligned} g(x+1, 0) &= 4q^{-1}g(x, 0) - g(x-1, 0) - 2g(x, 1), \\ g(x+1, y) &= 4q^{-1}g(x, y) - g(x-1, y) - g(x, y-1) - g(x, y+1), \quad y = 1, \dots, x-1, \\ g(x+1, x) &= 2q^{-1}g(x, x) - g(x, x-1). \end{aligned}$$

2.7. Simple cubic lattice

Green's function of the simple cubic lattice can be expressed in terms of the complete elliptic integrals multiplied by rational functions of Joyce's ξ variable [Joyce02] [lat3sc_q2xi, lat3sc_xi2q, lat3sc_xi2k]:

$$\xi^2 = \frac{1 - \sqrt{1 - q^2/9}}{1 + \sqrt{1 - q^2}}, \quad q = \frac{6\xi \sqrt{(1 - \xi^2)(1 - 9\xi^2)}}{1 - 9\xi^4}. \quad (2.24)$$

Formally the Green's function can be written in terms of \mathcal{K}^2 , \mathcal{E}^2 , and $\mathcal{K}\mathcal{E}$ with the argument given by $k_3(\xi)$ in Eq. (4.7). However, this basis is degenerate at $q = 0$, therefore we will use their combinations with different asymptotics at $\xi \rightarrow 0$:

$$\mathcal{K} \sim 1, \quad \mathcal{L} = \mathcal{K} - \mathcal{E} \sim 8\xi^3, \quad \mathcal{K}_1 = 8\xi^2\mathcal{K} - (1 - \xi)(1 + 3\xi^2)\mathcal{L} \sim 8\xi^2, \quad \mathcal{K}_2 = 8\xi^3\mathcal{K} - (1 - \xi)^2(1 - 3\xi^2)\mathcal{L} \sim 16\xi^4. \quad (2.25)$$

Now the basis (1.52) for recurrent evaluation of the Green's function and its derivatives can be written as [lat3scB]

$$h_0 = \frac{q}{6} \frac{(1 - 9\xi^4)}{(1 - \xi)^3(1 + 3\xi)} \mathcal{K}^2, \quad (2.26)$$

$$h_1 \equiv h_{(1,0,0)} = \frac{h_0}{q} - \frac{1}{6}, \quad (2.27)$$

$$h_2 \equiv h_{(1,1,0)} \frac{3}{64q} \frac{1}{(1 - 9\xi^4)} \left[\frac{\mathcal{K}_1^2}{(1 + \xi)(1 - 3\xi)} + \frac{(1 + 3\xi)\mathcal{K}_2^2}{\xi^2(1 - \xi)} \right] - \frac{2h_3}{q}, \quad (2.28)$$

$$h_3 \equiv h_{(1,1,1)} = \frac{3}{64} \frac{\mathcal{K}_1}{(1 + \xi)(1 - 3\xi)} \frac{\mathcal{K}_2}{\xi^2(1 - \xi)}. \quad (2.29)$$

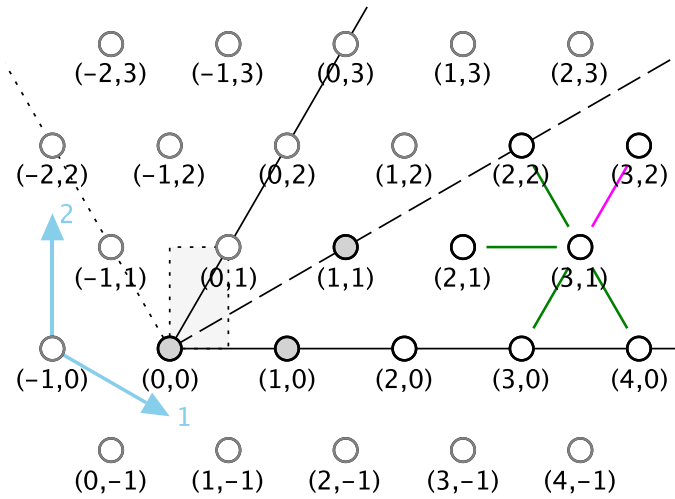


Figure 13: Triangular lattice coordinate system and notations. Cartesian vectors corresponding to k_1 and k_2 are shown as blue arrows. Recurrence scheme for evaluation of $g(3,2)$ is shown by colored bonds.

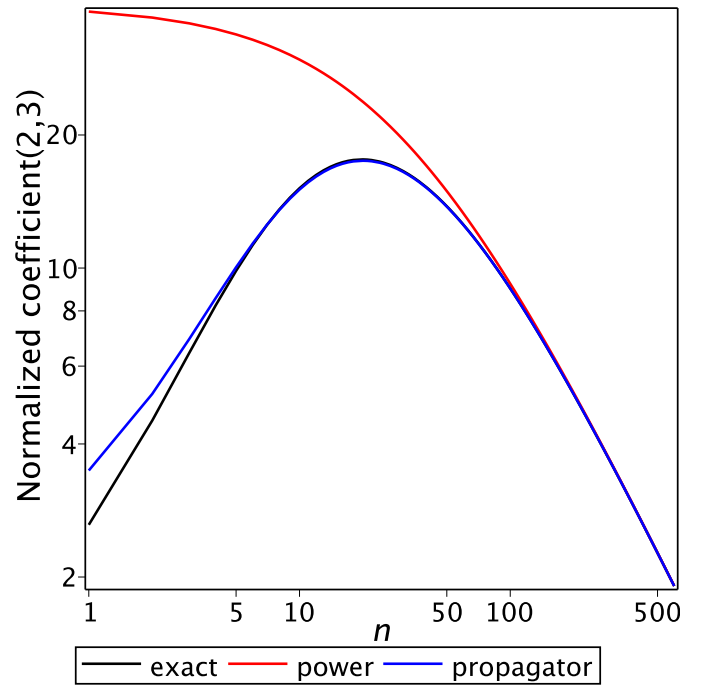


Figure 14: Two approximations of path expansion coefficients for triangular lattice.

Representation in terms of Heun G functions regular at $q = 0$ [Guttman10] [lat3scho_H0]:

$$h_0(q) = qH\left(9, \frac{3}{4}; \frac{1}{4}, \frac{3}{4}, 1, \frac{1}{2}; q^2\right)^2 \quad (2.30)$$

and at $q = 1$ [lat3scho_H1]:

$$h_0(q) = q\left[\sqrt{h_0(1)}H\left(-8, -\frac{9}{16}; \frac{1}{4}, \frac{3}{4}, \frac{1}{2}, 1; 1-q^2\right) - \frac{\sqrt{3(1-q^2)}}{8\pi\sqrt{h_0(1)}}H\left(-8, -\frac{69}{16}; \frac{3}{4}, \frac{5}{4}, \frac{3}{2}, 1; 1-q^2\right)\right]^2 \quad (2.31)$$

Value at $s = 0$ [Joyce02]:

$$\xi = \frac{\sqrt{2}-1}{\sqrt{3}}, \quad 1-9\xi^4 = 4\sqrt{2}(\sqrt{2}-1)^2, \quad (1-\xi)^2 = \frac{4}{3}\frac{\sqrt{3}-\sqrt{2}}{\sqrt{3}-1}, \quad (1-\xi)(1+3\xi) = \frac{4}{\sqrt{3}}\frac{\sqrt{2}-1}{\sqrt{3}-1}, \quad (2.32)$$

$$k = \frac{(\sqrt{2}-1)(\sqrt{3}-1)}{\sqrt{\sqrt{3}-\sqrt{2}}}, \quad h_0 = \frac{\sqrt{6}(\sqrt{2}+1)}{8}k^2\mathcal{K}^2 = \frac{\sqrt{3}-1}{192\pi^3}\Gamma\left(\frac{1}{24}\right)^2\Gamma\left(\frac{11}{24}\right)^2 \quad [\text{lat3scgo0}]. \quad (2.33)$$

§3. Other lattices

3.1. Triangular lattice

The Green's function of the triangular lattice was derived in Ref. [Horiguchi72]. A convenient coordinate system is shown in Fig. 13. In notations of Eq. (1.21), we chose the following bond vectors: $e^1 = e^{13}$, $e^2 = e^{23}$, $e^3 = e^{21}$. As common for hexagonal symmetry (and \mathbb{A}_d root system), each point (x, y) can be represented by a triple $(x_1, x_2, x_3) = (x, y, -x - y)$. In this representation the point symmetry of the lattice coincides with the symmetry of (x_1, x_2, x_3) with respect to permutations and inversion. In addition, the shortest-path distance to the origin is given by $|x| = \max_i |x_i|$, the Euclidean distance $\|x\|^2 = x^2 + y^2 + xy \equiv (\sum_i x_i^2)/2$, $V_1 = \sqrt{3}/2$, and $D = 3/2$. Alternative coordinate systems include the crystallographic one with b -axis oriented along $(-1, 1)$ direction and the rectangular one either body-centered or with missing sites (gray unit cell in

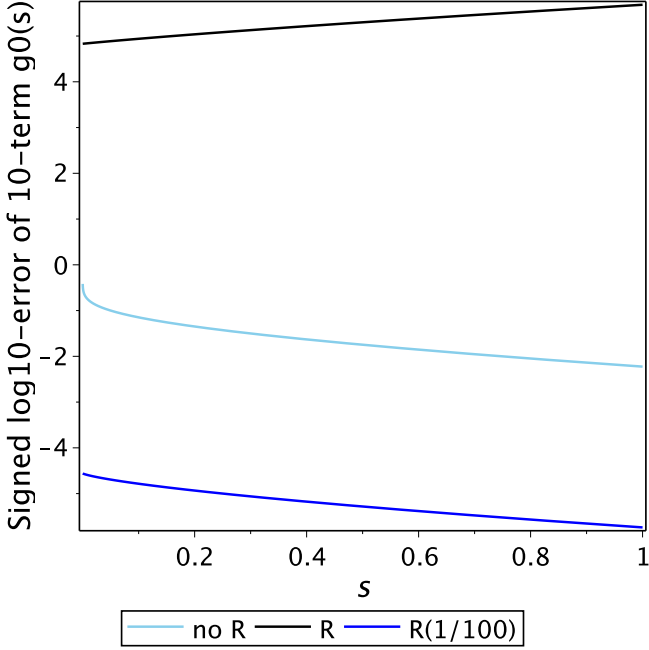


Figure 15: Error in evaluation of the Green's function of the triangular lattice at origin by path expansion.

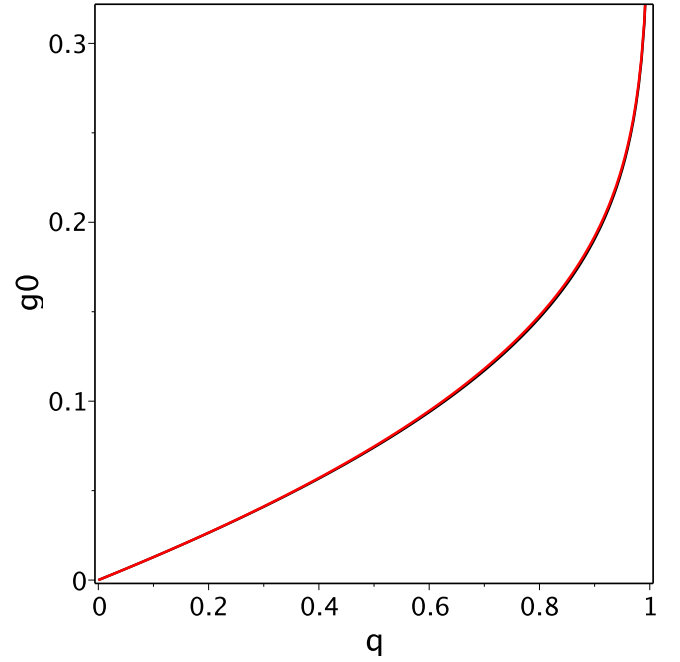


Figure 16: Approximation of the Green's function of the triangular lattice at origin by $q/8 + R_{0,1}^{\Phi}(q, \varepsilon_{\infty})$. The exact function is shown in black.

Fig. 13). The latter is used in Ref. [Horiguchi72]. Other uncommon notations of Ref. [Horiguchi72] include the rescaled Green's function $G = 2g$ and its argument $t = s/2 + 3$. The fundamental domain is defined by the inequality $0 \leq y \leq x$ and is marked by dash line in Fig. 13 as $1/12$ of the plane.

For the triangular lattice

$$S(k) = -6 + 2 \cos k_1 + 2 \cos k_2 + 2 \cos k_3, \quad k_3 = k_2 - k_1. \quad (3.1)$$

This band dispersion has three singularities: $S(0,0) = 0$, $S(\pi, \pi) = -8$, and $S(2\pi/3, -2\pi/3) = -9$. To compute "path expansion" coefficients, we substitute $k_1 = k'_1 + k'_2$, $k_2 = 2k'_2$ so that $k'_{1,2}$ are wave-vectors of a rectangular lattice. In these notations

$$S = -8 + 4(\cos k'_1 + \cos k'_2) \cos k'_2, \quad k_1 x + k_2 y = k'_1 x + k'_2 (x + 2y). \quad (3.2)$$

Now by using Eq. (1.36) we obtain

$$N_{(x,y)}(n) = \sum_{k=0}^{\lfloor n/2 \rfloor} \binom{n+|x|}{k, k+|x|} \binom{2(n-k)+|x|}{n-k+z}, \quad \left\{ \begin{matrix} |x| \\ z \end{matrix} \right\} = \left\{ \begin{matrix} \max \\ \min \end{matrix} \right\} (|x|, |y|, |x+y|), \quad (3.3)$$

with $q = 1/(1 + s/8)$ so that N is not the number of paths.

The Green's function can be written in terms of the complete elliptic integrals with the argument given by $k_3(\xi)$ in Eq. (4.7):

$$h_0 = \frac{\sqrt{\xi} k \mathcal{K}}{4}, \quad h_1 \equiv h_{(1,0)} = \left(\frac{4}{3q} - \frac{1}{3} \right) h_0 - \frac{1}{6}, \quad h_2 \equiv h_{(1,1)} = \left(\frac{8}{q^2} - \frac{20}{3q} - \frac{1}{3} \right) h_0 + \frac{1}{3} - \frac{\mathcal{E}}{2\sqrt{\xi} k}, \quad (3.4)$$

where

$$\xi^2 = \frac{q}{8+q} = \frac{1}{s+9}, \quad q = \frac{8\xi^2}{1-\xi^2}, \quad \text{so that } \sqrt{\xi} k \sim \frac{q}{2} \text{ at small } q \text{ and } \xi = \frac{1}{3} \text{ for } q = 1. \quad (3.5)$$

Density of states is given by

$$\rho(\sigma) = \frac{\sqrt{\xi}}{4\pi} \times \begin{cases} \mathcal{K}(1/k), & 0 \leq \sigma < 8 \quad (1/3 \leq \xi < 1), \\ k \mathcal{K}(k), & 8 < \sigma \leq 9 \quad (\xi > 1), \end{cases} \quad k = k(-\xi). \quad (3.6)$$

For symplectic honeycomb lattice (1.51) reduces to

$$\frac{1}{x_i} \sum_{j=1, j \neq i}^{d+1} D^{ij} g_x = \text{const}(i), \quad i = 1, \dots, d, \quad (3.7)$$

which for $d = 2$ in the selected above basis simplifies to

$$\frac{(D^1 - D^3)g_x}{x_1} = \frac{(D^2 + D^3)g_x}{x_2}. \quad (3.8)$$

By solving this equation with respect to one of D^i we exclude g_{x+e^i} from the Laplace equation and obtain the recurrence along one of the two remaining directions as illustrated in Fig. 13. In particular, for the recurrence along e^1 we obtain:

$$(x+y)g_{(x+1,y)} = (s+6)xg_{(x,y)} - (x-y)g_{(x-1,y)} - 2xg_{(x,y-1)} - (2x+y)g_{(x+1,y-1)} + yg_{(x-1,y+1)}. \quad (3.9)$$

The propagator can be obtained from Eq. (1.17):

$$\tilde{g}_{(x,y)}(t) = e^{-6t} \sum_{z \in \mathbb{Z}} I_{x+z}(2t) I_{y-z}(2t) I_z(2t). \quad (3.10)$$

3.2. Face-centered cubic lattice

For the site at the origin there are 12 nearest neighbors located at $\{\pm e^i, e^i \pm e^j\}$ in the unit vectors of the primitive cell or $\{\pm \frac{1}{2}e^i \pm \frac{1}{2}e^j\}$ in the unit vectors of the cubic cell. Let choose the cubic cell. Then

$$S(k) = -12 + 4 \cos \frac{k_2}{2} \cos \frac{k_3}{2} + 4 \cos \frac{k_3}{2} \cos \frac{k_1}{2} + 4 \cos \frac{k_1}{2} \cos \frac{k_2}{2}. \quad (3.11)$$

The no-integral formula for g_0 was obtained in [Morita71] and then improved in [Joyce94]:

$$g_0(s) = \frac{3}{\sqrt{16+s}(2\sqrt{12+s}+\sqrt{s})} \left[\frac{2}{\pi} K(k) \right]^2, \quad \text{where } k^2 = \frac{1}{2} \left(1 - \sqrt{\frac{s}{16+s}} \right) - \frac{12}{\sqrt{16+s}(2\sqrt{12+s}+\sqrt{s})}. \quad (3.12)$$

3.3. Diamond lattice

Diamond lattice consists of two fcc lattices: the first one has its origin at $(\frac{1}{8}, \frac{1}{8}, \frac{1}{8})$ in the cubic cell, and the second one is symmetric by the inversion. To use the lattice symmetry it is convenient to use the variable $a = s + 4$ instead of s . The solution of (1.13) is

$$\hat{g}(k) = \frac{\left(\begin{array}{c} a \\ 1 + e^{i\frac{k_2+k_3}{2}} + e^{i\frac{k_3+k_1}{2}} + e^{i\frac{k_1+k_2}{2}} \end{array} \quad \begin{array}{c} 1 + e^{-i\frac{k_2+k_3}{2}} + e^{-i\frac{k_3+k_1}{2}} + e^{-i\frac{k_1+k_2}{2}} \\ a \end{array} \right)}{a^2 - 4 - 4 \cos \frac{k_2}{2} \cos \frac{k_3}{2} - 4 \cos \frac{k_3}{2} \cos \frac{k_1}{2} - 4 \cos \frac{k_1}{2} \cos \frac{k_2}{2}}. \quad (3.13)$$

It is easy to see that

$$g_0^{11}(a) = a g_0^{\text{fcc}}(a^2 - 16) \equiv \frac{3}{2\sqrt{a^2-4} + \sqrt{a^2-16}} \left[\frac{2}{\pi} K(k) \right]^2, \quad (3.14)$$

where

$$k^2 = \frac{1}{2} + \frac{8-a^2}{2a^3} \sqrt{a^2-16} - \frac{8}{a^3} \sqrt{a^2-4}.$$

3.4. Body-centered cubic lattice

See [Morita71]

$$S(k) = -8 + 8 \cos k_1 \cos k_2 \cos k_3, \\ g_0(s) = \frac{1}{8+s} \left[\frac{2}{\pi} K(k) \right]^2, \quad \text{where } k^2 = \frac{1}{2} \left(1 - \sqrt{1 - \left(1 + \frac{s}{8} \right)^{-2}} \right).$$

3.5. Anisotropic lattices

For anisotropic hypercubic lattice

$$\tilde{g}_x(t) = \prod_{i=1}^d \exp \left[-(\alpha_i + \beta_i)t + \frac{1}{2} \ln \left(\frac{\alpha_i}{\beta_i} \right) x_i \right] I_{x_i} \left(2\sqrt{\alpha_i \beta_i t} \right),$$

where $\alpha_i = w_{x, x+e^i}$ and $\beta_i = w_{x, x-e^i}$. Some averages:

$$\langle x_i \rangle = (\alpha_i - \beta_i)t, \quad \langle \delta x_i^2 \rangle = (\alpha_i + \beta_i)t.$$

§4. Appendix

4.1. Some properties of finite difference operators

For any function f on \mathbb{Z} let us define the following finite difference operators:

$$(\partial^- f)_x = f_x - f_{x-1}, \quad (\partial^+ f)_x = f_{x+1} - f_x, \quad (\Delta f)_x = f_{x+1} + f_{x-1} - 2f_x.$$

Here are some identities:

$$(\partial^- f)_x = (\partial^+ f)_{x-1}, \quad (\partial^+ f)_x = (\partial^- f)_{x+1}, \quad \Delta f = \partial^- \partial^+ = \partial^+ \partial^- = \partial^+ - \partial^-.$$

If the summation is without boundaries then

$$\sum_x f_x (\partial^+ g)_x = - \sum_x g_x (\partial^- f)_x, \quad \sum_x f_x (\Delta g)_x = \sum_x g_x (\Delta f)_x.$$

But unlikely to the differential operators the finite difference of a product is more complicated:

$$\begin{aligned} \partial^\pm (fg)_x &= f_{x\pm 1} \partial^\pm g_x + g_x \partial^\pm f_x, \\ \partial^- (f \partial^+ g)_x &= f_x (g_{x+1} - g_x) - f_{x-1} (g_x - g_{x-1}), \\ \partial^+ (f \partial^- g)_x &= f_{x+1} (g_{x+1} - g_x) - f_x (g_x - g_{x-1}). \end{aligned}$$

For the hypercubic lattice, the function $G^{11}(x_1, \dots, x_d) = \Delta^1 g_{x_1 e^1 + \dots + x_d e^d}$ is symmetric with respect to change of sign at x_1 and is fully symmetric for the rest of arguments. The function $G^{12}(x_1, \dots, x_d) = \partial^1 \partial^{-2} g_{x_1 e^1 + \dots + x_d e^d}$ has special symmetry for the first two arguments and is fully symmetric for the rest of arguments, namely:

$$G^{12}(x_1, x_2, \dots) = -G^{12}(-x_1 - 1, x_2, \dots) = -G^{12}(x_1, -x_2 + 1, \dots) = G^{12}(x_2 - 1, x_1 + 1, \dots),$$

that matches the symmetry of the function $(x_1 + 1/2)(x_2 - 1/2)$.

4.2. Estimates and inequalities for Green's function for $s \geq 0$

For a general graph $0 < g_{xy} < g_{xx} < 1/s$.

For a primitive isotropic lattice ($w = 2\delta$)

$$s g_{e^1} + 2(\delta - 1)(g_{e^1} - g_{e^1 + e^2}) + (g_{e^1} - g_{2e^1}) = (g_0 - g_{e^1}).$$

From (1.34) it follows that $g_{e^1 + e^2} > g_{2e^1}$ and by combining this with the above identities we obtain the series of inequalities

$$\begin{aligned} \partial^2 g_{e^1} &< \partial^1 g_{e^1} < \partial^1 g_0 \equiv \frac{-\Delta^1 g_0}{\delta} \leq \frac{1}{2\delta}, & -\Delta^2 g_{e^1} &\leq \Delta^1 g_{e^1} < -\partial^1 \partial^{-2} g_0, \\ -\partial^1 \partial^{-2} g_0 &< \partial^1 g_0 \leq \frac{1}{2\delta}, & \Delta^1 g_{e^1} &\leq 2(\delta - 1) \partial^2 g_{e^1} < \frac{\delta - 1}{\delta(2\delta - 1)}, & -\Delta^2 g_{e^1} &= 2\partial^2 g_{e^1} < \frac{1}{\delta(2\delta - 1)}. \end{aligned}$$

4.3. Finite and semi-infinite one-dimensional lattices

For a ring of length L

$$g_x = \frac{\alpha}{1-\alpha^2} \frac{\alpha^x + \alpha^{L-x}}{1-\alpha^L} \equiv \frac{\cosh \kappa \left(x - \frac{L}{2}\right)}{2 \sinh \kappa \sinh \frac{\kappa L}{2}}, \quad x = 0, \dots, L-1. \quad (4.1)$$

The spectrum is

$$s_n = -4 \sin^2 \frac{\pi n}{L}, \quad n = 0, \dots, L-1,$$

and $s_{L-n} = s_n$.

For $X = \mathbb{Z}_+$

$$g_{yx} = \frac{\alpha}{1-\alpha^2} \left(\alpha^{|x-y|} + \alpha^{x+y+1} \right), \quad (4.2)$$

so that

$$\tilde{g}_{yx}(t) = e^{-2t} [I_{x-y}(2t) + I_{x+y+1}(2t)].$$

For a segment of length L

$$\begin{aligned} g_{yx} &= \frac{\alpha}{1-\alpha^2} \frac{\alpha^L}{1-\alpha^{2L}} \left(\alpha^{|x-y|-L} + \alpha^{L-|x-y|} + \alpha^{x+y+1-L} + \alpha^{L-1-x-y} \right) \\ &\equiv \frac{\cosh \kappa \left(L - x \vee y - \frac{1}{2}\right) \cosh \kappa \left(x \wedge y + \frac{1}{2}\right)}{\sinh \kappa \sinh \kappa L}, \quad x = 0, \dots, L-1. \end{aligned} \quad (4.3)$$

For an open segment of length L (particle is absorbed at $x = -1$ and $x = L$)

$$\begin{aligned} g_{yx} &= \frac{\alpha}{1-\alpha^2} \frac{\alpha^{L+1}}{1-\alpha^{2L+2}} \left(\alpha^{|x-y|-L-1} + \alpha^{L+1-|x-y|} - \alpha^{x+y+1-L} - \alpha^{L-1-x-y} \right) \\ &\equiv \frac{\sinh \kappa (L - x \vee y) \sinh \kappa (x \wedge y + 1)}{\sinh \kappa \sinh \kappa (L + 1)}, \quad x = 0, \dots, L-1. \end{aligned} \quad (4.4)$$

Note that

$$s \sum_{x=0}^{L-1} g_{yx} = 1 - \frac{\alpha^{y+1} + \alpha^{L-y}}{1 + \alpha^{L+1}}.$$

4.4. Some properties of complete elliptic integrals

Complete elliptic integrals allows for nontrivial changes of argument via modular transformations as discussed in [Joyce98] in relation to simple cubic Green's function. These transformation are performed with use of the elliptic modulus function $k^2(q) = (\theta_2(0, q)/\theta_3(0, q))^4$ and its inverse, nome function $q(k^2) = \exp(-\pi\mathcal{K}'/\mathcal{K})$, where prime denote complementary arguments and integrals. All elliptic integrals are rescaled by $2/\pi$:

$$\mathcal{K} \equiv \mathcal{K}(k) = \frac{2}{\pi} \mathbf{K}(k), \quad \mathcal{E} \equiv \mathcal{E}(k) = \frac{2}{\pi} \mathbf{E}(k). \quad (4.5)$$

An infinite series of modular transformations is defined by

$$k_n(q) = k(q^n), \quad \mathcal{K}_n = \mathcal{K}(k_n), \quad n \in \mathbb{N} \implies \frac{\mathcal{K}'_n}{\mathcal{K}_n} = n \frac{\mathcal{K}'_1}{\mathcal{K}_1}. \quad (4.6)$$

The case of $n = 3$ is considered in Ref. [Joyce98] using the parametrization

$$k_1^2 = \frac{16\xi}{(1-\xi)(1+3\xi)^3}, \quad k_3^2 = \frac{16\xi^3}{(1-\xi)^3(1+3\xi)}, \quad 0 \leq \xi < \frac{1}{3}, \quad (4.7)$$

so that

$$k_1'^2 = \left(\frac{1+\xi}{1-\xi} \right) \left(\frac{1-3\xi}{1+3\xi} \right)^3, \quad k_3'^2 = \left(\frac{1+\xi}{1-\xi} \right)^3 \left(\frac{1-3\xi}{1+3\xi} \right). \quad (4.8)$$

and

$$\frac{1-\xi}{1+3\xi} = {}_2F_1\left(-\frac{1}{6}, \frac{1}{2}; \frac{2}{3}, k_1^2\right)^2. \quad (4.9)$$

Then the following identities are valid:

$$\frac{k_3}{k_1} = \xi \frac{1+3\xi}{1-\xi}, \quad \frac{k'_3}{k'_1} = \frac{1+\xi}{1-\xi} \frac{1+3\xi}{1-3\xi}, \quad \sqrt{k_1 k_3} + \sqrt{k'_1 k'_3} = 1, \quad k_3 \mathcal{K}_3 = \xi k_1 \mathcal{K}_1 \quad (4.10)$$

For $\xi > 1/3$ the following two transformations, $t_{1,2}$ allows for the analytic continuation of the above formulas:

$$t_1(\xi) = \frac{1-\xi}{1+3\xi}, \quad t_2(\xi) = -\xi, \quad t_i(t_i(\xi)) = \xi, \quad i = 1, 2, \quad t_1(0) = 1, \quad t_1\left(\frac{1}{3}\right) = \frac{1}{3}. \quad (4.11)$$

The elliptic modulus transforms as follows:

$$k(\xi) k(\tilde{\xi}) = 1, \quad \frac{1}{k^2(\xi)} + \frac{1}{k^2(-\xi)} = 1 \iff k(-\xi) = i \frac{k(\xi)}{k'(\xi)}, \quad (4.12)$$

where $\tilde{\xi} = t_1(\xi)$ and k can be k_1 or k_3 here and below. Therefore, t_1 provides the analytic continuation to $1/3 < \xi < 1$ ($k^2 > 1$):

$$k \mathcal{K}(k \pm i0) = \mathcal{K}\left(\frac{1}{k}\right) \pm i \mathcal{K}'\left(\frac{1}{k}\right) \text{ for any } k, \quad \mathcal{K}'\left(\frac{1}{k(\xi)}\right) \equiv \mathcal{K}\left(\frac{1}{k(-\xi)}\right) \text{ for } \frac{1}{3} < \xi < 1, \quad (4.13)$$

whereas t_2 extends formulas to $\xi > 1$ ($k^2 < 0$):

$$\mathcal{K}(k) = k'(-\xi) \mathcal{K}(k(-\xi)). \quad (4.14)$$

4.5. Series at $s = 0$ for hypercubic lattice: implementation

Using the formulas

$$\begin{aligned} Z(\sqrt{z})' &= \left(\frac{d}{2} - 1\right) \frac{Z}{z} - \frac{z^{d/2-2}}{2} \chi_d, \quad \chi_d = \mathcal{I}\{d \text{ is even}\}, \\ -q^n (q^{1-n} f_n(q))' &= (n-1) f_n + 2(1-z) f'_n, \\ -q^n h'_n &= \left[(n-1)A_n + 2(1-z)A'_n - \chi_d(1-z)z^{d/2-2}B_n\right] + Z \left[(n-1)B_n + 2(1-z)B'_n + (d-2)(1/z-1)B_n\right], \end{aligned}$$

and expanding A and B in series:

$$\begin{aligned} \begin{Bmatrix} A_n \\ B_n \end{Bmatrix} &= \sum_{k=0}^{\infty} \begin{Bmatrix} a_{nk} \\ b_{nk} \end{Bmatrix} z^k, \\ (n-1)A + 2(1-z)A' &= \sum_{k=0}^{\infty} [(n-1-2k)a_k + 2(k+1)a_{k+1}] z^k \\ (1/z-1)B &= b_0/z + \sum_{k=0}^{\infty} (b_{k+1} - b_k) z^k \quad (\text{index } n \text{ is omitted for clarity}) \end{aligned}$$

we obtain recurrence relations for a_{nk} and b_{nk} . For the singular part, there is a secular equation for b_{n0} :

$$db_{n0} = nb_{n-1,0} + (d-n)b_{n+1,0} \implies b_{n0} = \text{const.}$$

The initial conditions (for the recurrence) $b_{n0} = 0$, $a_{0k} = \delta_{km}$, $k = 0, \dots, d-2$ generate $d-1$ regular solutions A_{mn} with $B = 0$, whereas the conditions $b_{n0} = 1$, $a_{0k} = 0$, $k = 0, \dots, d-2$ give the singular solution A_{dn}, B_{dn} . Note that in odd dimensions $A_{dn} = 0$ because $\chi_d = 0$.

Coefficients C_m for $d > 3$ can be determined either from $g_n(0)$ or $g_0^{(n)}(0)$. Also they can be determined from series of Ref. [Joyce03a]:

$$2h_0(q) = \sum_{k=0}^{\infty} C_k^J w_J^k + w_J^{d/2-1} \ln w_J \sum_{k=0}^{\infty} D_k^J w_J^k, \quad w_J \equiv w^{\text{Joyce}} = d(q^{-1} - 1).$$

Note that

$$\ln w_J = \ln \left[d \frac{1 - q^2}{q(1 + q)} \right] \implies p_0^J = \sqrt{\frac{d}{2}}.$$

Coefficients D_k^J can be calculated by the formula

$$D_k^J = \frac{(-1)^k a_k^J(d)}{(-2\pi)^{d/2} \Gamma(k + d/2)}, \quad \text{where} \quad {}_2F_0(1/2, 1/2; ; z/2)^d = \sum_{k=0}^{\infty} a_k^J(d) z^k.$$

References

- [Zhugayevych25a] A Zhugayevych, Efficient evaluation of lattice Green's functions, JPA 58, 025209 (2025)
- [Guttmann10] A J Guttmann, Lattice Green's functions in all dimensions, JPA 43, 305205 (2010)
- [Horiguchi72] T Horiguchi, Lattice Green's Functions for the Triangular and Honeycomb Lattices, JMP 13, 1411 (1972)
- [Joyce94] Joyce G S, On the cubic lattice Green functions, Proc R Soc Lond A 445, 463 (1994)
- [Joyce98] G Joyce, On the cubic modular transformation and the cubic lattice Green functions, JPA 31, 5105 (1998)
- [Joyce02] G Joyce, Exact evaluation of the simple cubic lattice Green function for a general lattice point, JPA 35, 9811 (2002)
- [Joyce03a] G Joyce, Singular behaviour of the lattice Green function for the d-dimensional hypercubic lattice, JPA 36, 911 (2003)
- [Maassarani00] Z Maassarani, Series expansions for lattice Green functions, JPA 33, 5675 (2000)
- [Morgan20] W Morgan, J Christensen, P Hamilton, J Jorgensen, B Campbell, G Hart, R Forcade, Generalized regular k-point grid generation on the fly, CMS 173, 109340 (2020)
- [Morita71] Morita T, Horiguchi T, Calculation of the lattice Green's function for the bcc, fcc, and rectangular lattices, JMP 12, 986 (1971)
- [Morita71b] T Morita, Useful procedure for computing the lattice Green's function - square, tetragonal, and bcc lattices, JMP 12, 1744 (1971)
- [Zucker11] I Zucker, 70+ Years of the Watson Integrals, JSP 145, 591 (2011)